F N P

Journal of FOOD PROCESS ENGINEERING

Edited by

D. R. HELDMAN

FOOD & NUTRITION PRESS, INC.
WESTPORT, CONNECTICUT 06881 USA

VOLUME 7, NUMBER 1 QUARTERLY

JOURNAL OF FOOD PROCESS ENGINEERING

All articles for publication and inquiries regarding publication should be sent to Prof. D. R. Heldman, Michigan State University, Department of Food Science and Human Nutrition, East Lansing, Michigan 48824 USA.

All subscriptions and inquiries regarding subscriptions should be sent to Food & Nutrition Press, Inc., 155 Post Road East, P.O. Box 71, Westport, Connecticut 06881 USA.

One volume of four issues will be published annually. The price for Volume 7 is $65.00 which includes postage to U.S., Canada, and Mexico. Subscriptions to other countries are $77.00 per year via surface mail, and $85.00 per year via airmail.

Subscriptions for individuals for their own personal use are $45.00 for Volume 7 which includes postage to U.S., Canada, and Mexico. Personal subscriptions to other countries are $57.00 per year via surface mail, and $65.00 per year via airmail. Subscriptions for individuals should be sent direct to the publisher and marked for personal use.

The *Journal of Food Process Engineering* (ISSN 0145-8876) is published quarterly (March, June, September and December) by Food & Nutrition Press, Inc.—Office of Publication is 155 Post Road East, P.O. Box 71, Westport, Connecticut 06881 USA. (Current issue is January 1984).

Second class postage paid at Westport, CT 06880.

POSTMASTER: Send address changes to Food & Nutrition Press, Inc., 155 Post Road East, P.O. Box 71, Westport, CT 06881.

JOURNAL OF FOOD PROCESS ENGINEERING

JOURNAL OF FOOD PROCESS ENGINEERING

Journal of
FOOD PROCESS ENGINEERING

VOLUME 7
NUMBER 1

Editor: D. R. HELDMAN

FOOD & NUTRITION PRESS, INC.
WESTPORT, CONNECTICUT 06881 USA

Food & Nutrition Press, Inc.
Westport, Connecticut USA

ISSN 0145-8876

Printed in the United States of America

CONTENTS

CONVECTIVE AND CONDUCTIVE EFFECTS OF HEAT TRANSFER IN POROUS MEDIA

JOSELITO V. DELA CRUZ[1]

Department of Grain Science and Industry
Kansas State University
Manhattan, Kansas 66506

RICHARD G. AKINS

Department of Chemical Engineering
Kansas State University
Manhattan, Kansas 66506

Received for Publication March 17, 1982
Accepted for Publication August 2, 1982

ABSTRACT

An experimental study was made of heat transfer by natural convection inside packed vertical cylinders whose wall temperatures varied sinusoidally with time. The packings were small glass or plastic spheres with water as the interstitial fluid. The purpose of this research was to stimulate, in a controlled laboratory model, the heat transfer to grain stored in bins.

Temperature distributions throughout the bed were determined for various sizes of packing, several height-to-diameter ratios, and for a number of frequencies of sinusoidal forcings. The results are presented graphically in terms of the amplitude ratios of the interior temperatures to the wall temperature and the phase lag between the interior and wall temperatures. The operating conditions ranged from essentially pure conduction to moderately strong natural convection.

The temperature distributions near the wall of the cylindrical container were found to be predicted by a simple one-dimensional model. Temperature distributions throughout an entire packed bed were quite complex when there was significant natural convection and, although general overall predictions were possible, accurate calculation of the temperature at a specific location and time was impossible.

---

[1]Present address: Dr. Joselito V. dela Cruz, Department of Agricultural Engineering, Central Luzon State Unviersity, Muñoz, Nueva Ecija, Republic of the Philippines

Journal of Food Process Engineering 7 (1983) 1–16.

INTRODUCTION

Natural convection is recognized as the macroscopic mechanism of moisture migration in a grain storage system. It was reported by Christensen (1974) that deterioration may occur in stored grain, even if it is initially at a safe and uniform moisture content, if there are marked differences in temperatures in different parts of the bulk. The intergranular air is generally not static, but is in motion due to convection caused by buoyant forces. Grain is hygroscopic, hence, moisture interchange takes place in the vapor phase when convection air currents move from a warm to cooler region. In spite of the recognition of its importance, most studies on heat transfer in stored grain (Bakshi and Bhatnagar 1972; Muir 1970; Yacuick *et al.* 1975; Bell 1978; Lo *et al.* 1975) have not dealt with the influence of natural convection.

Studies of convection in a horizontal porous medium by Horton and Rogers (1945), Morrison *et al.* (1949), and Rogers and Morrison (1950) showed that the minimum temperature gradient for which convection can occur is somewhat larger than that for a simple fluid as reported by Rayleigh (Elder 1967). The theoretical criterion for the onset of convection ($Ra > 4\pi^2$) has been verified by Combarnous and Bia (1971). They found a regular pattern of convective cells for low values of Ra (<260) and an unstable convective state for Ra higher than 260. The critical Ra for the onset of convective motion in a porous medium was reported to be 39.5 by Lawson and Yang (1975) and Lapwood (1948). Rhee *et al.* (1978) showed that increasing the depth of the liquid layer over the porous bed tended to lower the critical internal Ra at which the onset of convection occurred. For overlying liquid layer-to-bed depth ratios of one or more, natural convection was observed to begin at $Ra = 11.5$. The heat transfer data for $Ra > 11.5$ are correlated by

$$Nu = 0.19Ra^{0.69} \tag{1}$$

However, with no liquid layer on top of the bed, natural convection was observed to occur at $Ra = 46$, which is slightly higher than those observed in the earlier studies. Elder (1967) reported that for Rayleigh-type flow ($Ra > 40$) the heat transferred across the layer was independent of the thermal conductivity of the medium or depth of the layer.

The analysis of heat transfer through vertical surfaces to porous media has received considerably less attention than that for horizontal surfaces. Bejan (1980) found that a similarity regime (where the temperature and velocity profiles in the radial direction have the same shape regardless of vertical position) exists for $Ra(R/L)^2 \leq 11.8$. For values of $Ra(R/L)^2$ greater than about 200, the flow will be concentrated in a boundary layer

near the wall. Heat transfer in the similarity and boundary layer regimes was given as:

$$Nu = .255Ra(R/L)^2 \tag{2}$$

and

$$Nu = 5.62(R/L)\sqrt{Ra} \tag{3}$$

respectively. It is apparent that Eq. 2 agrees well with the relationship,

$$Nu = 0.181Ra^{0.51} \tag{4}$$

obtained by Bankvall as cited by Simpkins and Blythe (1980). Similarly, the methods of Simpkins and Blythe (1980) yielded

$$Nu = 0.186Ra^{0.5} \tag{5}$$

Several buoyancy driven boundary layer flows have been analyzed by Cheng and Chang (1976); Rudraiah and Nagaraj (1977); Rudraiah *et al.* (1980); and Dullien (1975) for the case of a Darcy flow. For flows beyond the validity of Darcy's law, Hanna *et al.* (1977) and Homsy and Sherwood (1976) pointed out that fluid loses its stability by buoyant and Taylor-Saffman modes. Plumb and Huenefeld (1981) characterized this flow by a modified Grashof number.

Grain and other agricultural products are most often stored in vertical-cylindrical bins, the walls of which are subjected to a combination of (more or less) cyclical temperature variations. The effects of these cyclical temperatures on heat transfer and the influence of natural convection are not well known. The irreproducibility of meteorological conditions and the very long periods of cycles make field data difficult to obtain and analyze. As a result, it was felt that studies of heat transfer in a model system of glass beads and water would help to demonstrate the nature of the heat transfer in the storage of grain. The model system has the advantage of examining several variables with adequate replications under controlled conditions. The time and space variations in temperature of the bed inside the cylindrical containers were measured under various sizes of spherical packing, cyclical temperature frequencies and container dimensions.

MATERIALS AND METHODS

The laboratory model was basically composed of a cylindrical container filled with glass beads and water. A programmable temperature

bath and a temperature measuring system, both computer controlled, were used. Fig. 1 shows a schematic diagram of the apparatus.

The cyclical wall temperature was produced by a computer-controlled bath surrounding the container. The 11.3 cm diameter by 30.5 cm high container was enclosed by a plexiglas box which served as the water bath. The bath temperature was monitored by a digital thermometer whose output was communicated (BCD) to a PDP 11/10 minicomputer. The computer, in turn, compared the actual bath temperature with the desired value and operated the bath control system to maintain the desired temperature. The temperature of the packed bed inside the container was measured by ten copper-constantan thermocouples located at different radial positions. All ten thermocouples could be moved vertically

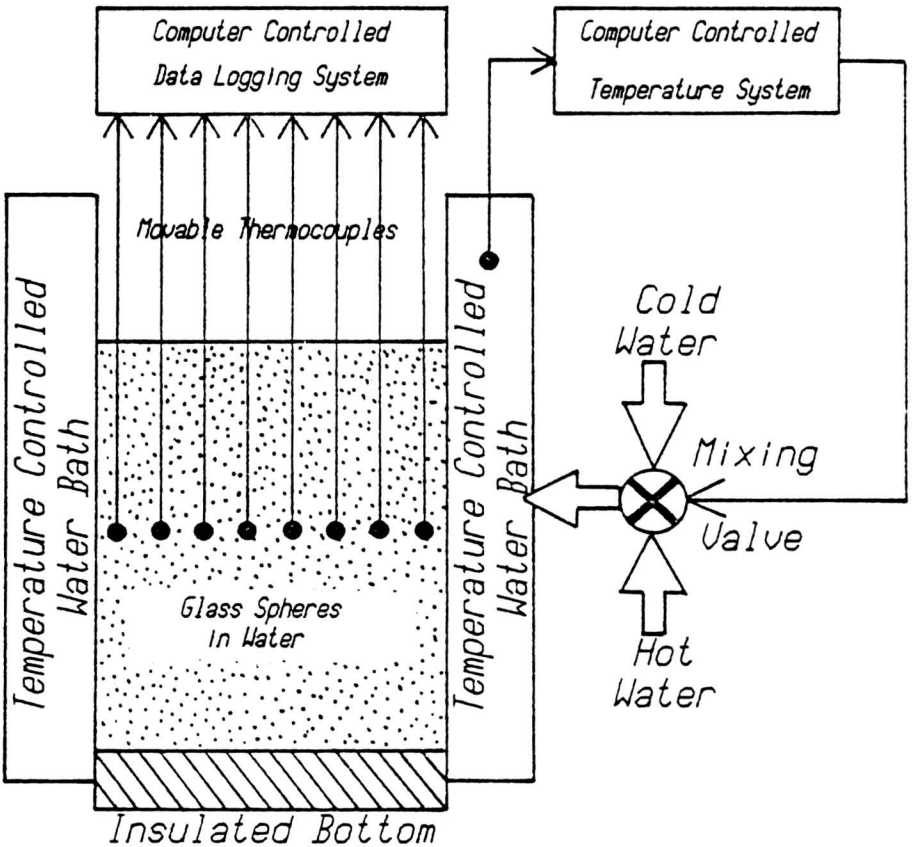

FIG. 1.. SCHEMATIC DIAGRAM OF THE EXPERIMENTAL GRAIN BIN MODEL AND MEASUREMENT SYSTEM

in the bed. The emf from each thermocouple was amplified in a multichannel amplifier. A multiplexer routed the selected analog signal to an analog-to-digital converter from which it was transmitted to the computer.

A run was initiated by allowing the cyclical temperature variations within the bed to become steady—about two to three cycles of temperature. Temperature data was then recorded at one vertical position in the bed for about 1½ cycles. The ten thermocouples were then moved to the next vertical position and data received for another 1½ cycles; and so on through the entire bed for that one frequency of wall temperature. The computer sampled a set of ten temperatures at a rate fast enough (less than one second) so that they could be assumed to represent instantaneous distributions. Details of the experimental apparatus and procedures may be found in the thesis by dela Cruz (1981).

Experiments were conducted for bin aspect ratios (height/diameter) of 0.5, 1.0, 1.5, and 2.0; frequencies of ½, 1, 2, 3, 4, 6, 8, 10, and 12 cycles per hour; and spherical bead sizes of 0.75, 4.0, 7.95, and 10.16 mm.

RESULTS AND DISCUSSION

A typical temperature response is shown in Fig. 2. The temperature at any point in the packed bed oscillated at the same frequency as the wall temperature, it was attenuated in amplitude, and it lagged behind the wall temperature. The temperature data was reduced to amplitude ratio, AR, and phase lag, ϕ, between the wall and inside temperature as indicated in the same figure.

In spite of the complex nature of the distributions discussed in the following sections, the data were quite reproducible for runs under identical conditions.

Effects of Aspect Ratio

Convective patterns were similar for all aspect ratios except 0.5 (Fig. 3 and 4). The iso-AR lines for the three higher aspect ratios were almost parallel to the wall and to one another for most of the height of the wall. However, they tended to converge towards the center as they reached the top of the bin. For an aspect ratio of 0.5 the contour lines were not parallel to the wall to as great an extent indicating that heat penetrated the upper portion of the short container much more quickly (i.e., high amplitude ratio and small phase lag) than in the taller cylinders. This also

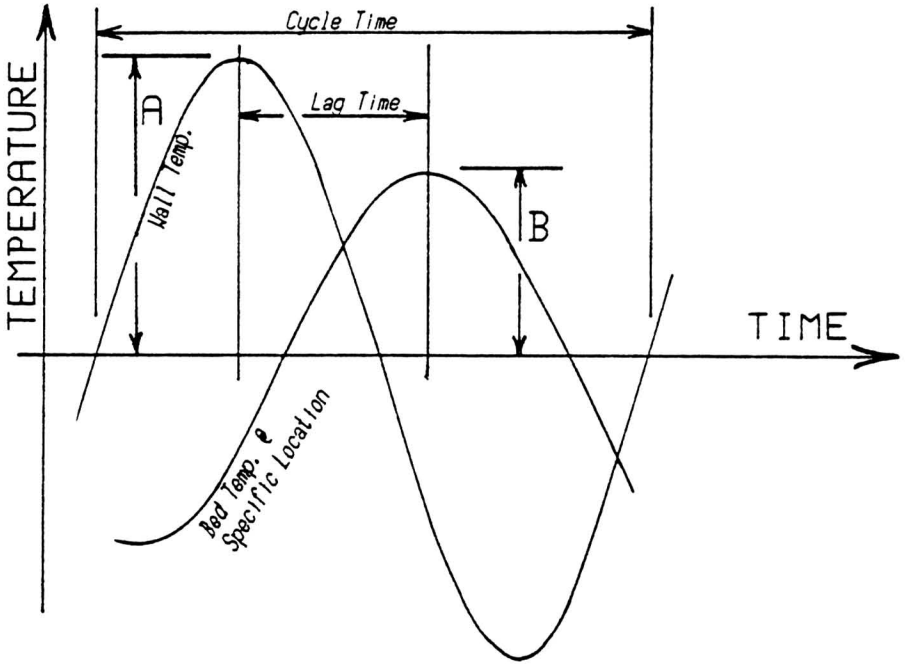

Amplitude Ratio, AR = B/A, (dimensionless)

Phase Lag, ϕ = (Lag Time)(360)/(Cycle Time), deg. of angle)

FIG. 2. GRAPHICAL REPRESENTATION OF THE TEMPERATURE VARIATION AT A SPECIFIC LOCATION INSIDE THE PACKED BED COMPARED WITH THE WALL TEMPERATURE VARIATION

means that temperature gradients in the axial direction of the tall cylinders were small compared to those in the radial direction except at the very top and bottom of the bin. This result was true when the cylinder had rather low permeability (small packings). Experiments in the next section examine the effects of the size of packing on the temperature distribution in the packed bed.

The fact that the shortest cylinder showed the most effects of natural convection may be somewhat surprising at first... one might expect taller cylinders to produce the largest natural convection flows. However, Bejan (1980) determined that the type of temperature distribution (i.e., similarity or boundary layer regime) is dependent on the value of $Ra(R/L)^2$. As the height decreases the distribution tends toward the

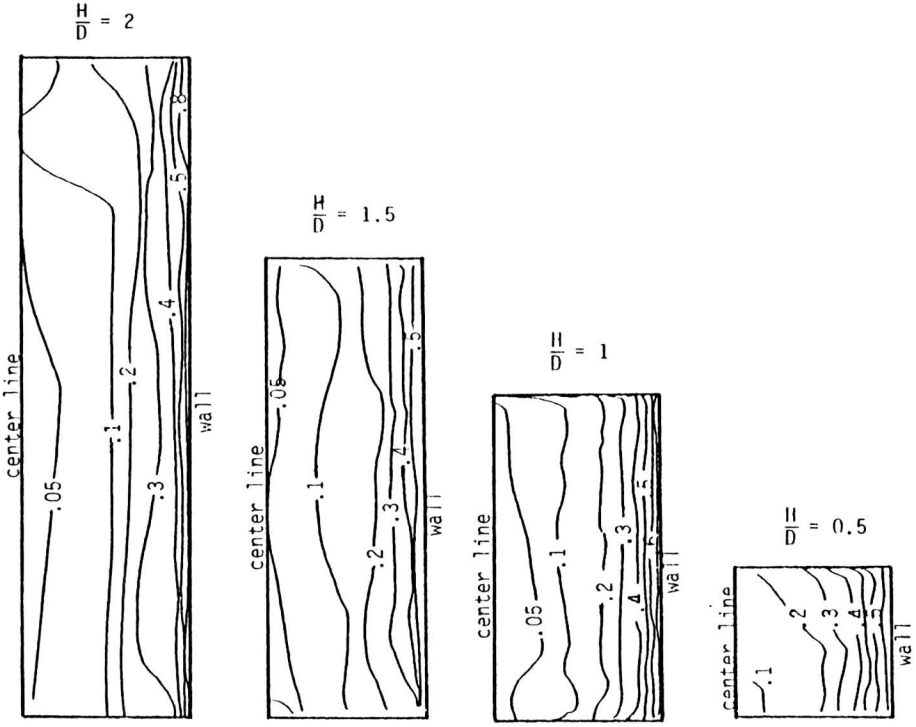

FIG. 3. THE EFFECTS OF ASPECT RATIO ON THE AMPLITUDE RATIO IN A CYLINDRICAL, PACKED CONTAINER
Frequency of imposed wall temperature = 4 cycles/hour.
Packing: 4 mm. glass beads in water.

boundary layer regime. Thus for shorter cylinders the effect of the boundary layer moving up the wall and across the top produces a marked increase in the heat penetration in the upper portions of the bed.

Effects of Spherical Packing Size

To determine the effects of the size of spherical packing on temperature distributions, the aspect ratio of the bin and the frequency of heating/cooling were kept constant at 1.0 and 4 cycles per hour, respectively. Four sphere sizes were studied: 0.75, 4.0, 7.95, and 10.16 mm. The data in Fig. 5 show that marked differences were observed in the contours (lines of the same AR and ϕ) as the permeability of the bed changed. Fig. 5 shows that the smaller the spheres, the lower the value of the AR and the larger the value of ϕ at any radial position.

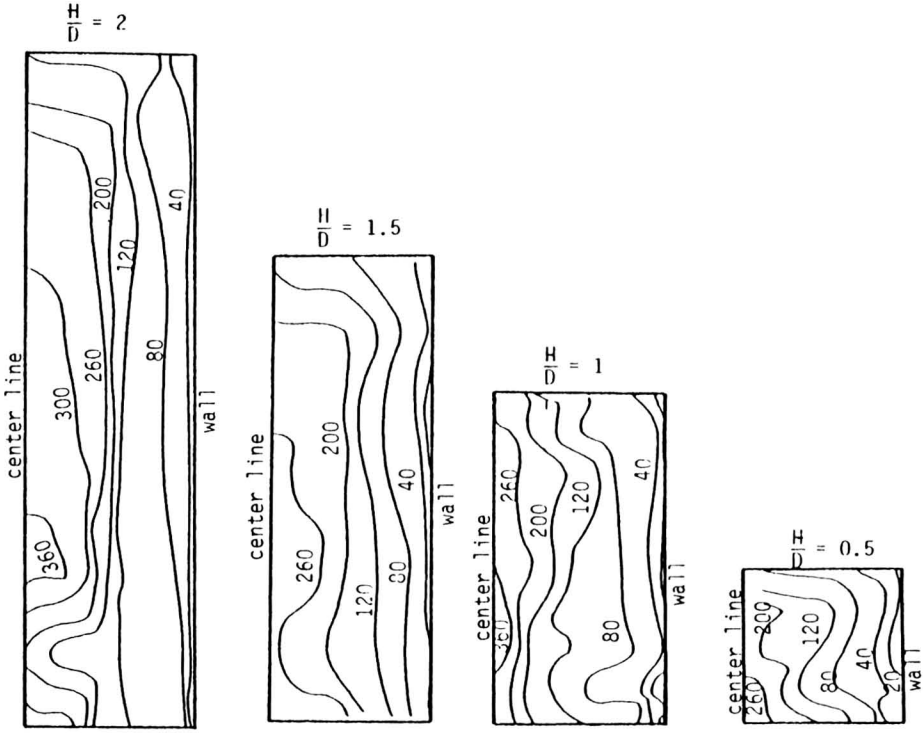

FIG. 4. THE PHASE LAG, IN DEGREES, BETWEEN INSIDE TEMPERATURES AND WALL TEMPERATURE FOR A CYLINDRICAL, PACKED CONTAINER
Frequency of wall temperature = 4 cycles/hour.
Packing: 4 mm glass beads in water.

In the bed packed with the smallest spheres (0.75 mm), the AR and ϕ values in the radial direction were similar at every vertical position. This is what would be expected for pure conduction or for the similarity regime in natural convection. In contrast, bins packed with 4 mm and larger spheres exhibited thermal patterns showing increased heat penetration, especially near the top. As the void spaces within a porous bed become smaller with smaller spheres, the frictional resistance to flow becomes larger and convective currents become smaller. In these experiments, the thermal conductivity of the fluid, water, and of the packing, glass, were approximately equal (0.63 and 0.76 W/m°K for water and glass, respectively) so that when conduction predominates, the contours are similar to that predicted for a solid glass cylinder (e.g., Fig. 5 for the 0.75 mm packing).

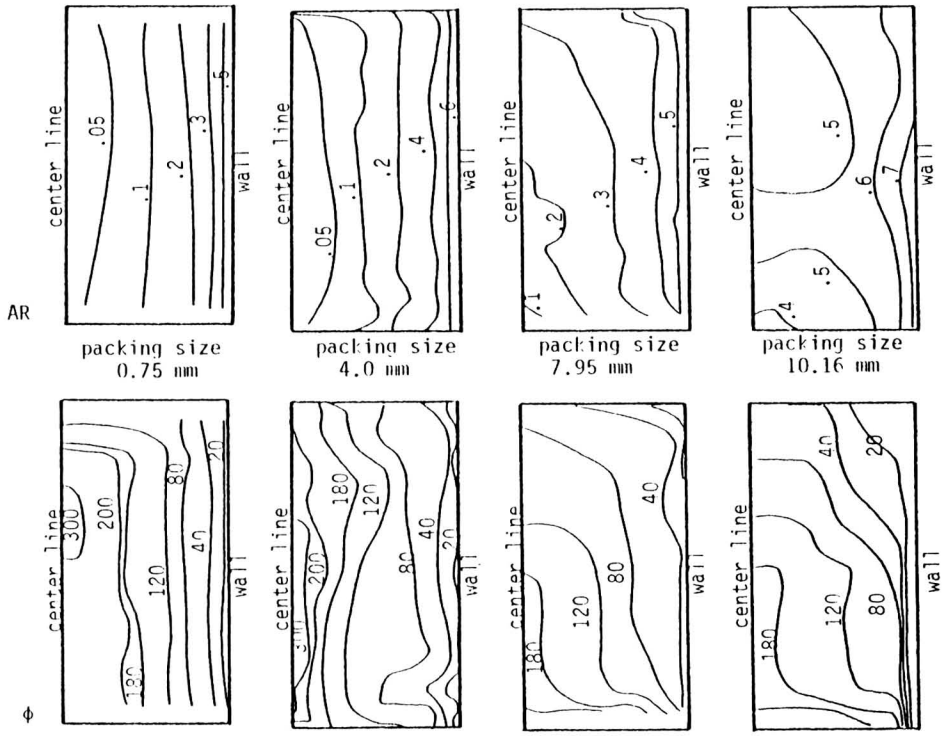

FIG. 5. THE EFFECT OF PACKING SIZE ON THE FREQUENCY RESPONSE INSIDE A CYLINDRICAL, PACKED BED
Frequency: 4 cycles/hour.
Aspect ratio: 1.0.

Effects of Frequency

Fig. 6 shows the effects of varying the frequency of the wall temperature on the AR and ϕ in a cylinder with aspect ratio of 1.5 and containing 4.0 mm spheres. The data in Fig. 6 were obtained using a mean temperature of 36°C and an amplitude of ±3°C. As the frequency of heating/cooling was increased from 0.5 to 12 cycles per hour, AR decreased across the bin whereas the ϕ is increased.

In Fig. 6, it is illustrative to examine the two extremes of heating/cooling frequency. At 0.5 cycle per hour, the AR contours in the radial direction show a value of 0.6–0.7 at the center. In contrast, at 12 cycles per hour, AR is less than 0.05 at the center of the cylinder. This shows that at high frequencies, the heat penetrated only near the wall of the

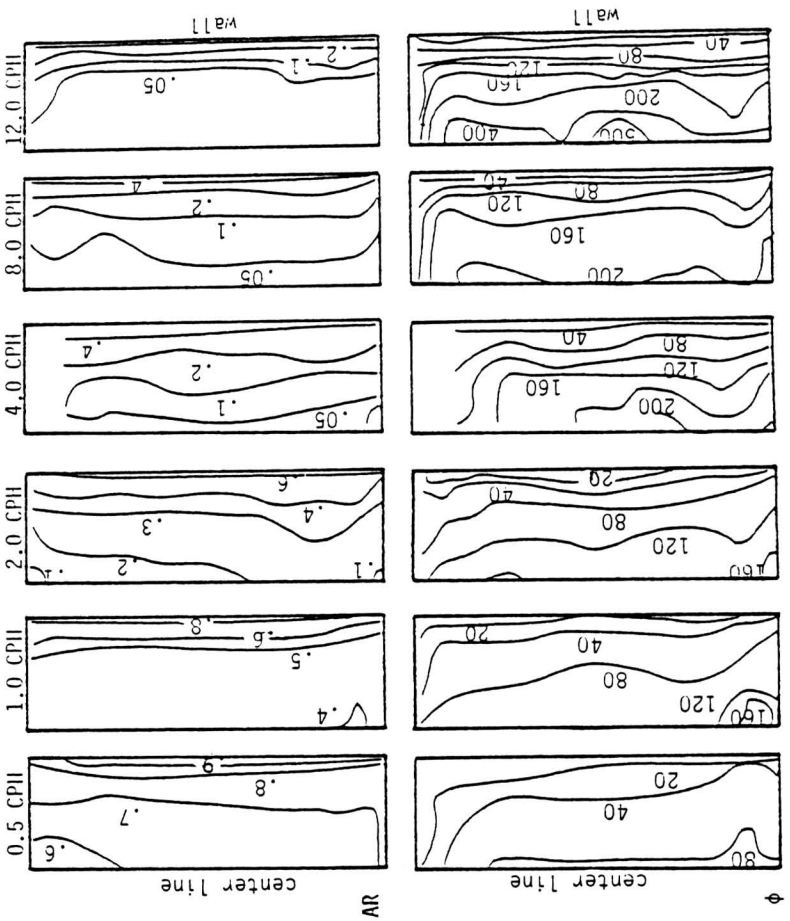

FIG. 6. AMPLITUDE RATIOS AND PHASE LAGS BETWEEN THE INSIDE TEMPERATURES AND THE WALL TEMPERATURE AS A FUNCTION OF FREQUENCY
Packing: 4 mm glass beads. Aspect ratio: 1.5

cylinder. The remainder of the contents responded, essentially, only to the mean temperature. The ϕ data in Fig. 6 verify this: at 0.5 cycle per hour, the temperature in the center of the cylinder lagged the temperature of the wall by 0.22 cycles (80°), whereas at 12 cycles per hour, the lag was 1.4 cycles (500°). Obviously, little heat was penetrating the center of the cylinder at higher frequencies.

Comparison with Previous Work

Plumb and Huenefeld (1981) studied the non-Darcy natural convection from vertical heated surfaces of different geometrical configurations in saturated porous media. Their findings demonstrated the relative importance of inertial effects which were characterized by a modified Grashof number, Gr'

$$Gr' = \frac{g\beta KK'(T_w - T_\infty)}{\nu^2}$$

where

$$K = \frac{D_p^2 \epsilon^3}{150(1-\epsilon)^2}$$

and

$$K' = \frac{1.75 D_p}{150(1-\epsilon)}$$

The functional relationship between Gr' and heat transfer is shown in Fig. 7. For values of Gr' up to 0.1, the heat transfer through vertical heated surfaces deviates from that assuming Darcy's law by less than 5% but drops off rapidly as Gr' increases beyond 0.1. The inertial effects should be incorporated in the analysis for $Gr' > 0.1$ (Plumb and Huenefeld 1981).

The modified Grashof number, the Darcy-Rayleigh number, and $Ra(R/L)^2$ for each packing are given in Table 1. The values were calculated using one-half the amplitude as ΔT and an H/D ratio of 1. Also included in the table are the values for wheat in air under the same conditions of ΔT and H/D. As the table values show, inertial effects were not very important and the experiments ranged from essentially no convection to the boundary-layer regime.

For wheat in upright concrete silos, Converse *et al.* (1973) analytically studied the transient heat transfer in stored grain and compared their

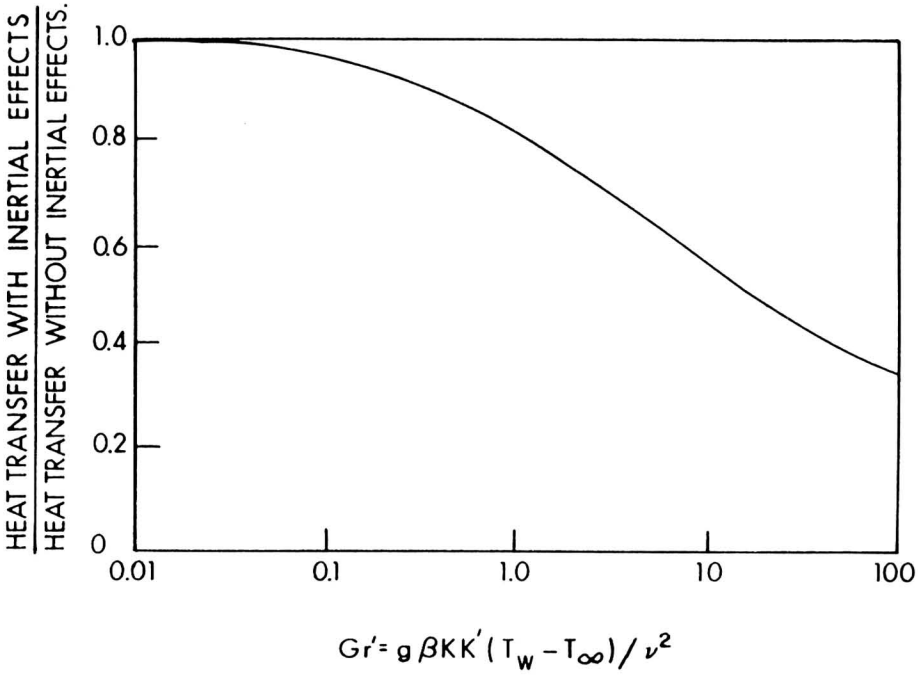

FIG. 7. THE RATIO OF HEAT TRANSFER WITH INERTIAL EFFECTS TO THAT WITH NO INERTIAL EFFECTS AS A FUNCTION OF THE PARAMETER, GR′
(Plumb and Huenefeld 1981)

Table 1. Dimensionless Parameters Assuming ΔT = (Amplitude/2) and H/D = 1

Packing Size, mm	Gr'	Ra	$Ra(R/L)^2$
0.75, glass spheres	4.2×10^{-5}	2	.68
[a]2.90, wheat (in air)	4.6×10^{-2}	.25	.09
4.00, glass spheres	6.4×10^{-3}	56	19
7.95, glass spheres	5.2×10^{-2}	230	79
10.16, hollow plastic spheres	1.1×10^{-1}	370	130

[a]Added for comparison

results with experimental data. Using their methods, the amplitude ratio and phase lag between the wall and the inside temperatures of the cylinder were calculated. Fig. 8 presents the comparison of AR and ϕ obtained from this study and those from the analytical methods of Converse at 7 cycles per hour. The graphs of the experimental results of

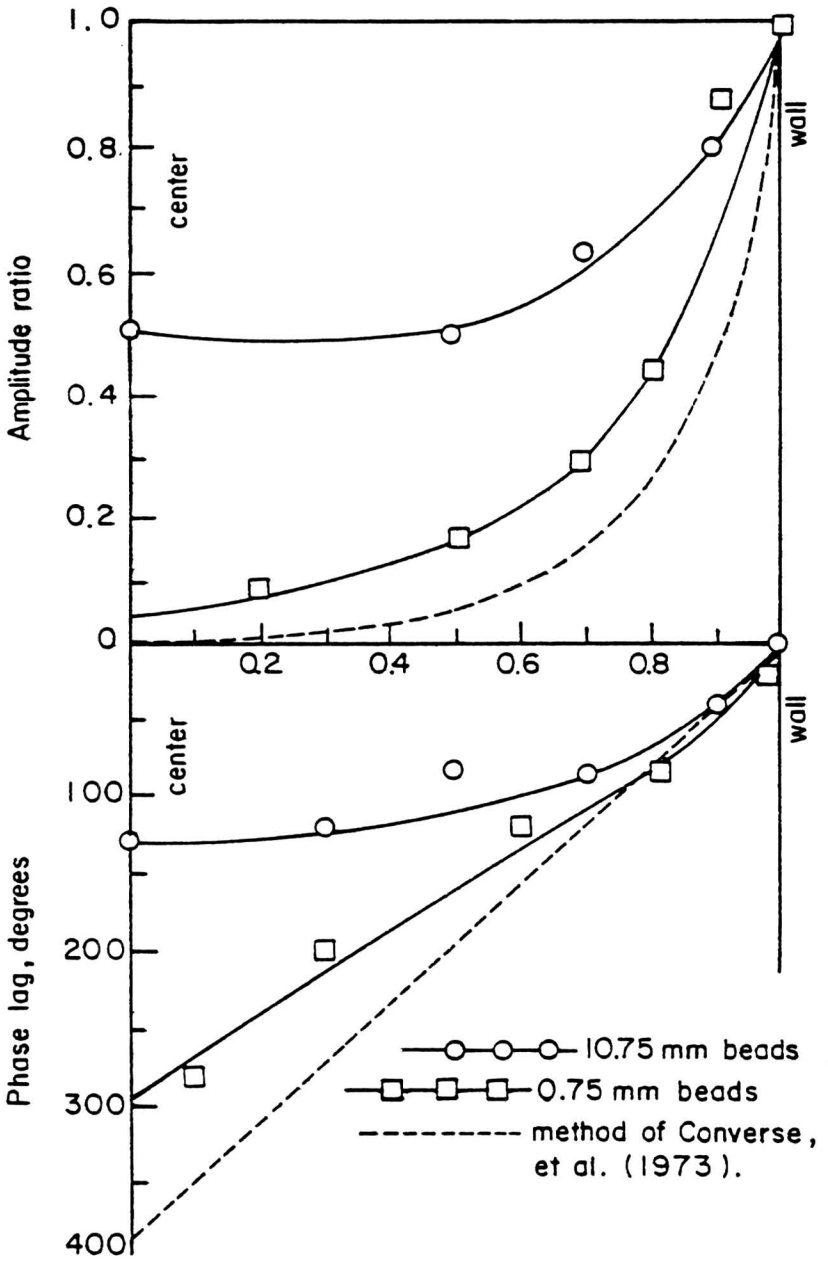

FIG. 8. COMPARISON OF AMPLITUDE RATIO AND PHASE LAG OBTAINED FROM THE PRESENT STUDY AND THAT USING THE METHOD OF CONVERSE *et al.* (1973) AT 4 CYCLES PER HOUR

this study were based on the data obtained from the middle section (vertically) of the model bin. The close agreement between the experimental results with 0.75 mm spheres and those of Converse indicates conduction is the predominant mode of heat transfer. On the other hand, the higher AR and lower ϕ with 10.16 mm spherical packing showed the important role of natural convection.

For the conditions of this study, the AR and ϕ may be approximated within $\pm 10\%$ near the wall by assuming pure convection with a weighted average thermal diffusivity. For example, Labs (1979) developed an equation for yearly periodic cycles in soils which, when applied to this work, gave predictions of AR which were 3 to 10% high in the region within 5 mm of the wall.

SUMMARY AND CONCLUSIONS

An experimental laboratory study of heat transfer to a cylinder packed with spherical particles was conducted to gain insight into temperature distributions in stored food products. The laboratory model provided controllable and repeatable experimental conditions which could not have been obtained in actual grain storage.

The conclusions which may be drawn from this study are:

(1) The temperature distributions within packed beds due to fluctuations in wall temperature may be extremely complex because of natural convection and prediction of exact temperature levels and changes may be considerably in error.

(2) Conduction is the predominant mechanism of heat transfer in packed beds with permeabilities similar to that of wheat.

(3) Even so, some convection is evident and, although small compared to conduction, it may have considerable influence on moisture migration.

(4) Natural convection becomes quite important for packings much larger than wheat.

NOMENCLATURE

A = mean temperature, °C
AR = amplitude ratio, dimensionless
B = amplitude, °C
D = diameter, m
Gr' = modified Grashof number, $g\beta KK'(T_w - T_\infty)/\nu^2$, dimensionless
g = acceleration due to gravity, m/s^2

h = height, m
k = thermal conductivity, W/m °K
K = permeability expressed in terms of characteristic pore diameter and porosity, m^2
K' = transport property related to inertial effect, m
Nu = Nusselt number, hL/k, dimensionless
R = radius, m
r = radial position, m
Ra = Darcy-Rayleigh number, $g\beta\Delta TKL/\nu\alpha$, dimensionless
T = temperature, °C or °K

GREEK SYMBOLS

α = thermal diffusivity, m^2/s
β = coefficient of thermal or cubical expansion, $°K^{-1}$
Δ = difference
ϵ = void fraction, porosity, dimensionless
μ = viscosity, kg/m s
ν = kinematic viscosity, m^2/s
ϕ = phase lag, degrees

REFERENCES

BAKSHI, A. S. and BHATNAGAR, A. P. 1972. Temperature study in grain storage bins. J. Agric. Engg. Res. *9*(2), 30–42.

BEJAN, A. 1980. Natural convection in a vertical cylindrical well filled with porous medium. Int. J. Heat Mass Trans. *23*(5), 726–729.

BELL, K. A. 1978. A simulation model of temperature in grain bins. Australia National University. Australia. M. Sc. Thesis.

CHENG, P. and CHANG, I. 1976. Buoyancy induced flows in a saturated porous medium adjacent to impermeable horizontal surfaces. Int. J. Heat Mass Trans. *19*(11), 1267–1272.

CHRISTENSEN, C. M. 1974. *Storage of Cereal Grains and Their Products.* AACC, Inc. St. Paul, Minnesota.

COMBARNOUS, M. A. and BIA, P. 1971. Combined free and forced convection in porous media. Soc. of Petroleum Engrs. *11*(4), 399–405.

CONVERSE, H. H., GRAVES, A. H. and CHUNG, D. S. 1973. Transient heat transfer within wheat stored in a cylindrical bin. Trans. of the ASAE. *16*(1), 129–133.

DELA CRUZ, J. V. 1981. Heat Transfer by Natural Convection in Stored Grains. Kansas State University Ph.D. Thesis. 178 pp.

DULLIEN, F. A. L. 1975. Single phase flow through porous media and pore structure. Invited Review. The Chem. Eng. J. *10*, 1–34.

ELDER, J. W. 1967. Steady free convection in a porous medium. Fluid Mechanics. *27*(1), 29-48.

ELDER, J. W. 1967. Transient convection in a porous medium. J. Fluid Mechanics. *27*(3), 609-623.

HANNA, M. R., KOZICKI, W. and TIU, C. 1977. Flow of drag reducing fluids through packed beds. The Chem. Eng. J. *13*(2), 93-99.

HOMSY, G. M. and SHERWOOD, A. E. 1976. Convective instabilities in porous media with through flow. AIChE J. *22*(1), 168-174.

HORTON, C. W. and ROBERS, F. T., JR. 1945. Convection currents in a porous medium. J. Applied Physics. *16*(6), 367-370.

LABS, K. 1979. Underground building climate. Paper presented in a Workshop on the Design, Sizing, Calculation, Construction and Marketing of Passive Solar Heated Buildings. Passive Solar Associates, Kansas City, Missouri.

LAPWOOD, E. R. 1948. Convection of a fluid in a porous medium. Proc. of the Cambridge Philosophical Societies. *44*(4), 508-521.

LAWSON, M. L. and YANG, W. 1975. Thermal stability of binary gas mixtures in a porous medium. J. Heat Transfer. Trans. of the ASME. *97*(3), 378-381.

LO, K. M., CHEN, C. S., CLAYTON, J. T. and ADRIAN, D. D. 1975. Simulation of temperature and moisture changes in wheat storage due to weather variability. J. Agric. Eng. Res. *20*(1), 47-53.

MORRISON, H. L., ROGERS, F. T., JR. and HORTON, C. W. 1949. Convection currents in porous media. II. Observation on conditions of onset of convection. J. Applied Physics. *20*(11), 1027-1029.

MUIR, W. E. 1970. Temperatures in grain bins. Can. Agric. Engg. *12*(1), 21-24.

PLUMB, O. A. and HUENEFELD, J. C. 1981. Non-Darcy natural convection from heated surfaces in saturated porous media. Int. J. Heat Mass Trans. *24*(5), 765-768.

ROGERS, F. T. JR. and MORRISON, H. L. 1950. Convection currents in porous media. III. Extended theory of critical gradient. J. of Applied Phys. *21*(12), 1476-1479.

RHEE, S. J., DHIR, V. K. and CATTON, I. 1978. Natural convection heat transfer in beds of inductively heated particles. J. of Heat Transfer. Trans. of the ASME. *100*(1), 78-84.

RUDRAIAH, N. and NAGARAJ, S. T. 1977. Natural convection through vertical porous stratum. Int. J. Engg. Sci. *15*, 589-600.

RUDRAIAH, N., VEERAPA, B. and RAO, S. B. 1980. Effects of nonuniform thermal graident and adiabatic boundaries on convection in porous media. J. Heat Transfer. Trans. of the ASME. *102*(2), 254-259.

SIMPKINS, P. G. and BLYTHE, P. A. 1980. Convection in a porous layer. Int. J. Heat Mass Trans. *23*(8), 1069-1078.

YACUICK, G., MUIR, W. E. and SINHA, R. N. 1975. A simulation model of temperatures in stored grain. J. Agric. Eng. Res. *20*(3), 245-258.

HEAT TRANSFER TO WATER AND SOME HIGHLY VISCOUS FOOD SYSTEMS IN A WATER-COOLED SCRAPED SURFACE HEAT EXCHANGER

L. B. J. VAN BOXTEL and R. L. DE FIELLIETTAZ GOETHART

Institute CIVO-Technology TNO
P. O. Box 360
3700 AJ ZEIST
The Netherlands

Received for Publication July 29, 1982
Accepted for Publication November 29, 1982

ABSTRACT

Heat transfer in a water-cooled scraped surface heat exchanger has been investigated. The overall heat transfer coefficient in the heat exchanger is composed of three elements: heat transfer coefficient in the coolant jacket, resistance to heat flow in the separation wall and heat transfer coefficient inside the scraped cylinder.

A method for assessing the heat transfer coefficient at the coolant side was developed.

In contrast with studies published elsewhere, heat transfer was investigated with food systems which are non-newtonian and possess a complicated and unknown flowing behavior at higher shear rates.

For water and three starch-based food products (starch content 12–18%) the heat transfer coefficients inside the scraped cylinder were measured for shaft speeds ranging from 1.67 to 10 revolutions/s. The experimental results were compared with heat transfer coefficients calculated with a model based on the penetration theory. For the starch-based products, in general, no consistent interactions between mass flow rates and internal heat transfer coefficients were observed. In the shaft speed range studied heat transfer coefficients at scraped surface varied from 3200 to 7800 W/m^2K for water, from 500 to 3150 W/m^2K for velouté sauce, from 670 to 1330 W/m^2K for roux and from 780 to 1900 W/m^2K for ragout.

INTRODUCTION

Heat transfer to flowing products is a frequently applied operation in the food industry. Particularly in this industry it is not practical to heat

Journal of Food Process Engineering 7 (1983) 17–35.

or cool certain products in conventional plate or tubular heat exchangers, on account of their viscous character. Moreover, if heat-sensitive products are heated in such an equipment, for instance for sterilization, they may deteriorate on the heated surface. Heat transfer is often impeded by the formation of a stagnant layer at the heat transferring surface and can be improved by continuously scraping the surface. In this way formation of a stagnant film is obviated and the rotation results in the scraped off layer continuously mixing with the bulk, while fresh material is moved to the heated or cooled wall. This mechanically induced convective transport improves heat transfer.

This paper describes some aspects of the heat transfer phenomena in a water-cooled scraped surface heat exchanger (further referred to as SSHE). In the first instance experiments with water in the product-cylinder of the SSHE were carried out. The aim of these experiments was to determine the heat transfer coefficient at coolant side as a function of the cooling water flow rate in the jacket. The second part concerns cooling experiments with three food products, i.e., velouté sauce, roux and ragout. These are highly viscous products of non-newtonian nature and ragout even contains small pieces of solid meat. The influence of the type of product and of operating conditions on heat transfer at the scraped wall side were items of interest in this study.

THEORETICAL CONSIDERATIONS

General

The physico-technical aspects of heat transfer, design considerations and applications of SSHE's have been described by several authors (Houlton 1944; Skelland *et al.* 1962; Latinen 1959; Harriot 1959; Trommelen 1967; 1970; Trommelen *et al.* 1971; Anton 1977 and Cuevas & Cheryan 1980). The most elaborate investigations on heat transfer in SSHE's using newtonian flowing glycerol-water mixtures are those reported by Skelland *et al.* (1962) and Trommelen (1970). The basic principles of heat transfer can be applied to a SSHE just as well as to other forms of heat transfer equipment. Assuming that a plug flow consists of coolant and product, the heat flow from scraped side to cooling jacket is defined with the formula:

$$q = U \cdot A \cdot \Delta T_{\ln} \tag{1}$$

In this relation the heat transferring area A is based on the logarithmic mean radius $R_{\ln}$ of the cylindrical heat transferring wall:

$$A = 2\pi \cdot L \cdot R_{\ln} = 2\pi \cdot L \cdot \frac{R_e - R_i}{\ln R_e/R_i} \tag{2}$$

The overall heat transfer coefficient U used in formula (1) is composed of three terms, as expressed by the resistance equation:

$$\frac{1}{U} = \frac{R_{\ln}}{R_i} \cdot \frac{1}{h_s} + \frac{R_e - R_i}{k_w} + \frac{R_{\ln}}{R_e} \cdot \frac{1}{h_j} \tag{3}$$

In the SSHE under study $R_{\ln}/R_i$ (1.01) and $R_{\ln}/R_e$ (0.98) approach unity. In this case it is justified to simplify formula (3), without significant loss in accuracy, to:

$$\frac{1}{U} = \frac{1}{h_s} + \frac{x}{k_w} + \frac{1}{h_j} \tag{4}$$

in which x is the thickness of the heat transferring wall.

Using $\Delta T_{\ln}$ in formula (1) implies that in the evaluation of the overall heat transfer coefficient U axial dispersion or backmixing effects are neglected.

Physical Aspects of Heat Transfer at Product Side

Skelland *et al.* (1962) performed an extensive experimental study on heat transfer in a Votator. Based on a dimensional analysis they determined the dimensionless groups which should be included in a correlation for heat transfer at product side. Their cooling experiments with glycerol-water mixtures could be correlated by means of the dimensionless equation:

$$\frac{h_s \cdot d_t}{k_p} = \alpha \left(\frac{c_p \cdot \mu_p}{k_p} \right)^{\beta} \cdot \left(\frac{(d_t - d_s) \cdot v_p \cdot \rho_p}{\mu_p} \right)^{1.00} \cdot \left(\frac{d_t \cdot N}{v_p} \right)^{0.62} \cdot \left(\frac{d_s}{d_t} \right)^{0.55} \cdot n^{0.53} \tag{5}$$

where for cooling viscous liquids α is 0.014 and β is 0.96 and for cooling thin mobile liquids α is 0.039 and β is 0.70. The formulated equation is not satisfactory in every respect; the choice of the dimensionless groups is rather arbitrary and the determination of the exponents is debatable. Moreover, the influence of the heat conductivity on the heat transfer coefficient is of minor significance in the relationship ($h_s \sim k_p^{-0.04}$),

although the mechanism of heat transfer for viscous fluids will be largely based on conduction (Trommelen 1967, 1970). A more fundamental approach is given by Latinen (1959) and Harriott (1959). Their model is based on the penetration theory from which they derived a theoretical relationship for the heat transfer coefficient:

$$h_s = 1.13(k_p \cdot \rho_p \cdot c_p \cdot N \cdot n)^{0.5} \tag{6}$$

Application of this correlation in experiments with viscous fluids (Trommelen 1970) showed deviations between theoretical and experimental results. The conclusion must be that the mechanism is more complicated than suggested by the penetration model. For water the theoretical and experimental values did match, while for more viscous fluids the experimental values were lower than expected. Trommelen (1970) suggested to describe the heat transfer by an equation resulting from the penetration theory modified by an empirically determined correction factor ϕ:

$$h_s = 1.13(k_p \cdot \rho_p \cdot c_p \cdot N \cdot n)^{0.5} \cdot \phi \tag{7}$$

Heat Transfer Coefficient in the Water-Cooled Jacket

The heat transfer coefficient at coolant side in SSHE's was calculated by other authors (Houlton 1944; Skelland *et al.* 1962; Trommelen 1970) with the Dittus Boelter formula:

$$Nu = 0.0225 Re^{0.8} \cdot Pr^{0.4} \tag{8}$$

in which the characteristic length in Nu and Re is the hydraulic diameter. Originally this formula was developed for calculating film heat transfer coefficients in tubular heat exchangers under turbulent flow conditions. The above mentioned authors used this relationship also for estimating heat transfer coefficients for the helical path in the cooling jacket. For assessing the actual heat transfer coefficients in the water cooled jacket in our SSHE we followed a different procedure. If the rotation speed of the shaft is varied and the remaining conditions are unchanged then $h_s \sim N^{0.5}$ follows from the penetration theory (formula 7). However, this is conditional upon the correction factor ϕ being independent of the shaft speed, which is expected to be true for water as the product treated in the SSHE (Trommelen 1970; Harriott 1959). Combining this with formula 4 results in:

$$\frac{1}{U} = \frac{1}{C \cdot N^{0.5}} + \frac{x}{k_w} + \frac{1}{h_j} \tag{9}$$

(C is a constant; k_w/x is 8889 W/m^{2}K for the SSHE in question)

From experiments with water in the product cylinder and a given constant coolwater flow rate the overall heat transfer coefficient U as a function of shaft speed can be calculated. Plotting U^{-1} values versus $N^{-0.5}$ theoretically leads to a linear relationship. Extrapolating U^{-1} to $N^{-0.5}$ is zero results in a value from which the actual heat transfer coefficient in the jacket can be estimated.

MATERIALS AND METHODS

Equipment

A vertical type scraped surface heat exchanger (CREPACO VT-422; Crepaco Inc., Chicago, USA) was used for the heat transfer measurements. Cooling water and product were fed into the SSHE at the bottom section and flowed co-currently to the topsection. Two rows of scraper blades were mounted on the shaft, which was driven by a hydraulic motor with an infinitely variable speed. Details of the SSHE-equipment are listed in Table 1.

The number of revolutions of the shaft could be varied between 0 and 10 rev/s and was measured with a flashlight stroboscope. Tap water was used as coolant. The product for the cooling experiments was prepared in a cooking vessel. From there it was pumped by means of a variable hydraulically driven lobe pump through an automatically controlled,

Table 1. Details of scraped surface heat exchanger

Shaft diameter (d_s)	: 38.0×10^{-3} m
Internal diameter scraped wall ($d_i = 2R_i$)	: 98.0×10^{-3} m
External diameter scraped wall ($2R_e$)	: 101.6×10^{-3} m
Thickness heat transferring scraped wall (x)	: 1.8×10^{-3} m
Axial length scraped wall (L)	: 510.0×10^{-3} m
Logarithmic mean area heat transferring wall (A)	: 0.16 m^2
Rows of mounted scraper blades	: 2
Jacket cooling water helix: depth (δ)	: 4.2×10^{-3} m
width (y)	: 80.0×10^{-3} m
Hydraulic diameter jacket cooling helix (d_h)	: 8.0×10^{-3} m
Thermal conductivity wall material	: 16 W/mK

steam-heated SSHE-cylinder connected in series to heat the product to about 70–95°C before entering the water-cooled cylinder under investigation. Temperatures of cooling water and product in- and outlet were measured in line with copper-constantan thermocouples and registered on a temperature-recorder (Philips PM8235-multipoint recorder). Mass flow rate of cooling water and product were measured by weighing a suitable amount having passed through the SSHE for a certain time. When the steady state for an experimental run had been established, mass flow rates, shaft speed, inlet and outlet temperatures were recorded. Heat flow was calculated from enthalpy changes in coolant or cooled product. The overall heat transfer coefficient was determined with formula (1).

Product Formulations and Physical Properties

For the experimental work the following products were used: water, velouté sauce, roux and ragout. The composition and the relevant physical properties of the last three food systems are given in Table 2. The density and the specific heat for the starch products were calculated on the basis of literature values found for the recipe components water, flour, fat and beef. The thermal conductivities were obtained from heat penetration tests (temperature range 20–80°C), carried out by the authors.

The starch-based products were prepared as follows: fat was melted and heated to 80°C in a steam-heated, mixing cooking vessel, flour was added and mixed to a homogeneous mass with the melted fat; hot water and in the case of ragout the meat cut in small pieces were added; the mass was heated to 95°C and kept at this temperature for at least 4 min before starting the cooling experiments.

The food systems have, after cooking, a firm consistency due to gelati-

Table 2. Composition and physical properties of the food products

	Composition (%)				Physical Properties		
	Water	Flour	Fat	Meat[1]	ρ_p (kg/m^3)	c_p (J/kg K)	k_p (W/mK)
Velouté sauce	82.0	12.0	6.0	—	1000	3760	0.56
Roux	73.0	18.0	9.0	—	1000	3550	0.50
Ragout	66.4	16.3	8.2	9.1	1000	3520	0.50

[1]Cooked beef cut in small pieces

nation of the starch. Velouté sauce, the most mobile of the three, showed a pronounced pseudoplastic flowing behavior. The apparent viscosities measured in a rotoviscosimeter (Contraves Rheomat 15 T) at three temperature levels are given in Table 3.

For roux and ragout no reliable viscosities could be measured in the rotoviscometer. The viscosities are in any case considerably higher than for velouté sauce.

Levels of Experimental Conditions

The ranges of the operating conditions and some calculated axial and rotational Reynolds numbers are summarized in Table 4. The ranges of the product inlet and outlet temperatures are also included in order to give an idea of the performance of the cooling section of the SSHE. Due to lack of clearness with respect to the viscosity behavior inside the SSHE the axial and rotational Reynolds numbers are very uncertain for the

Table 3. Apparent viscosities for velouté sauce

Shear Rate (s^{-1})	Apparent Viscosity (Ns/m^2)		
	35°C	60°C	85°C
2.927	30.9	18.0	17.8
6.779	17.2	10.4	9.9
30.38	6.3	4.0	3.5
59.22	4.1	2.6	2.2

Table 4. Ranges of experimental conditions

Experimental Condition	Product/Food System			
	Water	Velouté	Roux	Ragout
Mass flow rate product (kg/s)	0.076–0.084	0.032–0.114	0.017–0.112	0.035–0.103
Shaft speed (s^{-1})	1.67–10.00	1.67–9.92	1.67–8.33	1.67–8.33
Product inlet temperature (°C)	95	95	70–80	70–82
Product outlet temperature (°C)	41.2–55.7	29.3–83.4	19.0–61.0	29.2–62.4
Axial Reynolds number Re_a	1760–1950	0.1–0.4[1]	—	—
Rotational Reynolds number Re_r	41300–226000	6–37[1]	—	—

[1]Based on an apparent viscosity of 2.6 Ns/m^2 (60°C; shear rate 59.22 s^{-1})

starch-based food products. For velouté these values are estimated on the basis of a measured apparent viscosity at 60°C and a shear rate of 59.22 s^{-1}. For roux and ragout the relevant values will undoubtedly be lower than for velouté sauce.

RESULTS AND DISCUSSION

Heat Transfer in the Water-Cooled SSHE-Jacket

Six cooling experiments with water in the product cylinder were carried out, using various cooling-water flow rates (ranges 0.171–0.417 kg/s). In each of the experiments the shaft speed was varied (range 1.67–10 rev/s). The resulting overall heat transfer coefficients were based on the total heat flow calculated with the formula: $q = \phi_p \cdot c_p \cdot \Delta T_p$. Due to the greater temperature difference the heat flow calculated on the basis of the temperature change of the product (ΔT_p) is more accurate than when based on temperature change of the coolant (ΔT_c).

The inverses of the overall heat transfer coefficients (U^{-1}) of each experiment were plotted versus $N^{-0.5}$ (method described under "Theoretical considerations"). Plotting in this way resulted in straight lines for all six cooling-water rates (correlation coefficients between 0.991 and 0.997). Two plots are shown in Fig. 1.

The assumption that h_s is proportional to $N^{0.5}$ seems to be justified. The resulting heat transfer coefficients in the water-cooled jacket are presented in Table 5.

The cooling-water flow is turbulent in all situations (Reynolds number ranging from 3571 to 8709). Since the flow in the jacket is turbulent, the film coefficient of heat transfer was expected to be proportional to the velocity to the power 0.8. The six film coefficients obtained were transformed to Nusselt numbers and plotted in Fig. 2 versus $Re^{0.8} \cdot Pr^{0.4}$ (physical properties of water based on observed mean temperatures).

The experimental heat transfer coefficients of the SSHE under investigation were fitted best square to a line expressed with the equation (correlation coefficient 0.974):

$$Nu = 0.0158 Re^{0.8} \cdot Pr^{0.4} + 18.2 \qquad (10)$$

The values are close to the one predicted by the Dittus Boelter Eq. (8). A maximum deviation of circa 10% appears at the lower *Re*-numbers. In the following experiments the heat transfer coefficients in the jacket were calculated with the empirical Eq. (10).

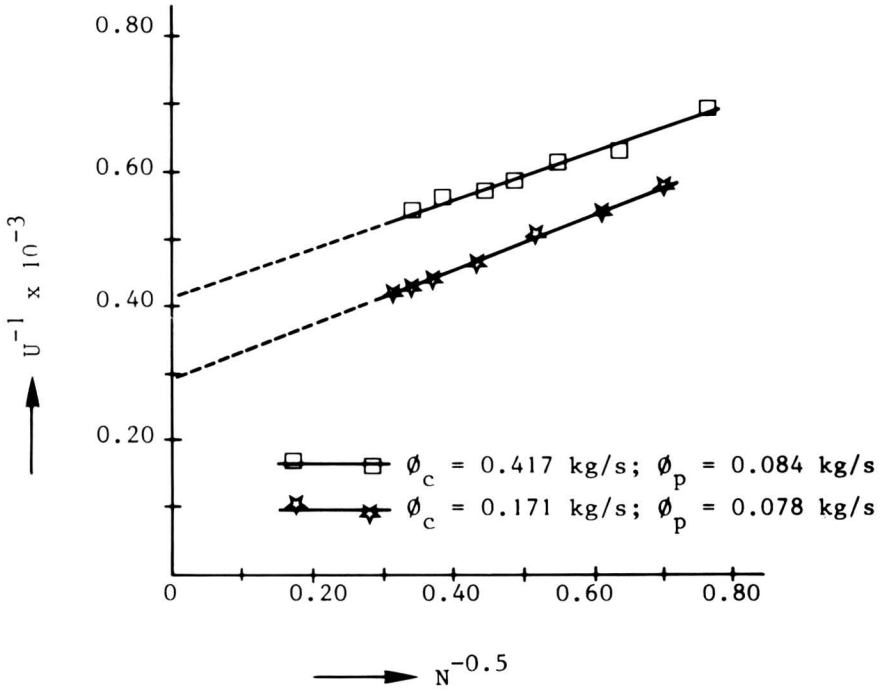

FIG. 1. OVERALL HEAT TRANSFER COEFFICIENT AS A FUNCTION OF SHAFT SPEED DURING A CONSTANT FLOW OF WATER IN PRODUCT-CYLINDER (ϕ_p) AND JACKET (ϕ_c)

Influence of Shaft Speed on Heat Transfer to Water at the Scraped Surface

Using the known h_j and wall resistance, the overall heat transfer coefficients for the experiments with water were converted into heat transfer coefficients at the scraped surface. The empirical correction factor ϕ followed from the ratio experimental h_s-value and the expected value of the penetration theory (see formula 7). The shaft speed dependence of h_s is given in Fig. 3.

Heat transfer coefficients at scraped surfaces ranged from 3200 to 7800 W/m^{2}K. The correction factor ϕ fluctuated around unity. There was no significant influence of the shaft speed on ϕ (see Fig. 4).

Effects such as incomplete mixing of the scraped layer with the bulk, which could affect heat transfer adversely, were not observed with a low viscous fluid like water. Harriott (1959) found also for water a value of ϕ near one.

Table 5. Experimental heat transfer coefficient in the jacket as a function of the cooling water flow

Mass Flow Rate Cooling Water ϕ_c (kg/s)	Heat Transfer Coefficient Jacket h_j (W/m^{2}K)
0.417	5572
0.410	5451
0.330	4458
0.250	4027
0.204	3964
0.171	3220

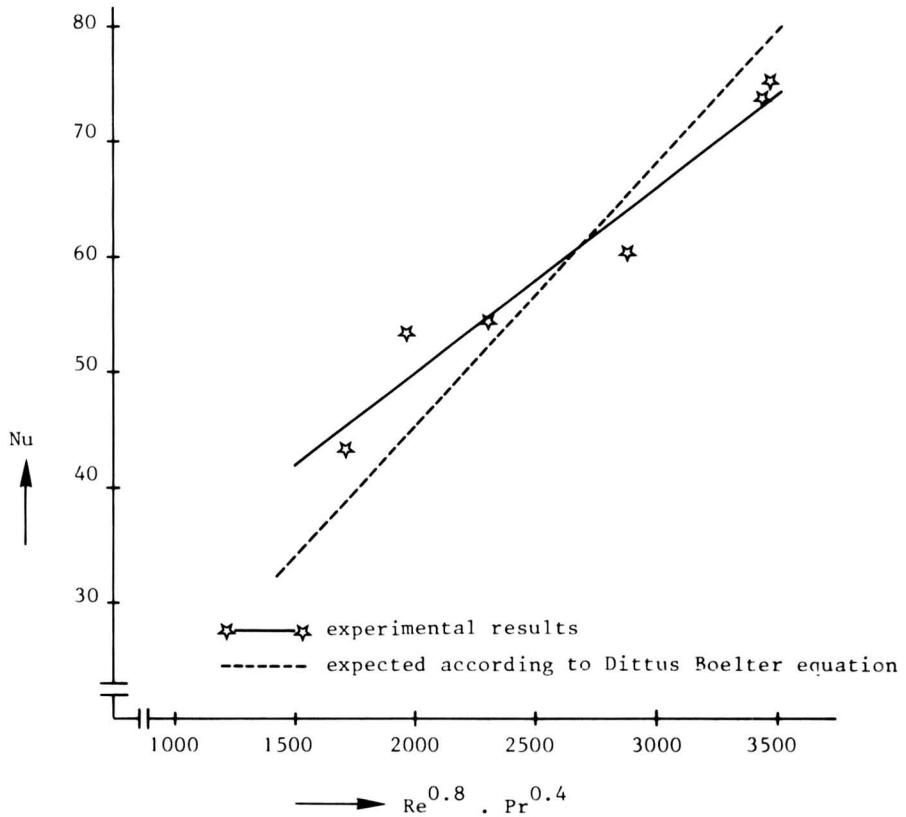

FIG. 2. HEAT TRANSFER IN THE WATER-COOLED JACKET IN DIMENSIONLESS GROUPS

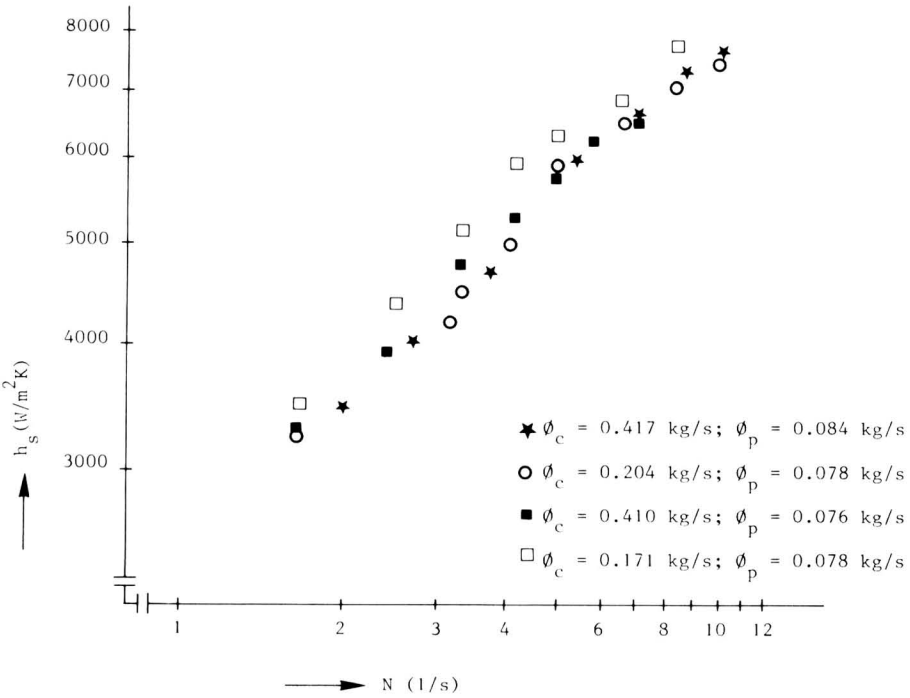

FIG. 3. INFLUENCE OF SHAFT SPEED ON HEAT TRANSFER COEFFICIENT AT SCRAPED SURFACE SIDE
Product: water

Heat Transfer at Scraped Surface. Experiments with Velouté Sauce, Roux and Ragout

During the experimental work with the food products some difficulties arose. Due to the heavy consistency, the product was not completely mixed when leaving the SSHE, which made it impossible to accurately measure the average outlet temperature. In some experiments also an unknown part of the fat-fraction of the product crystallized when the temperature sank to below 40°C. For reasons already mentioned, the heat flow calculations were based on temperature change of the cooling-water. A moderate cooling water flow rate of about 0.2 kg/s was used to allow for the temperature difference to be measured with sufficient accuracy.

Velouté sauce. The heat transfer coefficients at the scraped surface increased for this product from 500 W/m^{2}K at a shaft speed of 1.67 rev/s to 3150 W/m^{2}K at 10 rev/s (see Fig. 5).

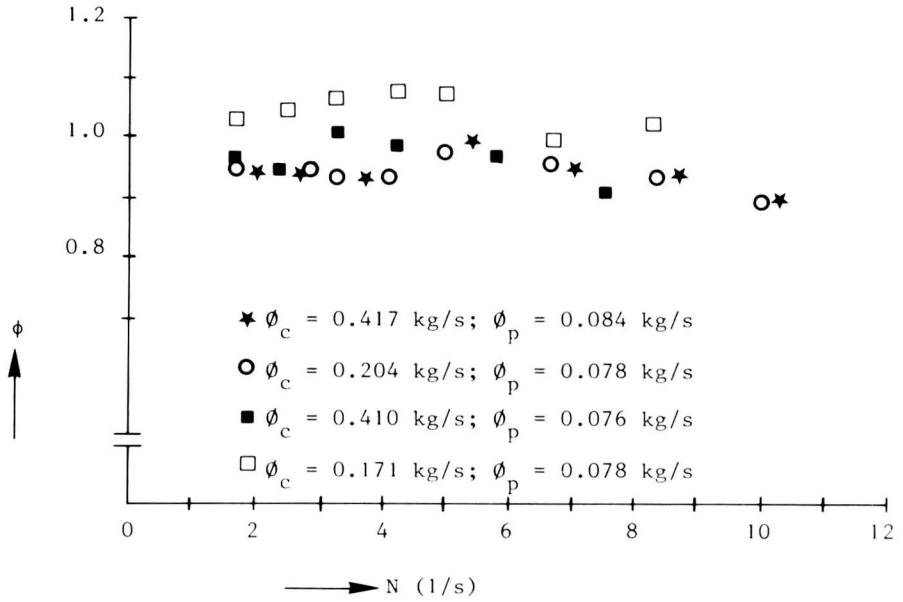

FIG. 4. INFLUENCE OF THE SHAFT SPEED ON EMPIRICAL CORRECTION FACTOR ϕ
Product: water

No clear interaction effect of mass flow rate and shaft speed could be observed. The empirical correction factor ϕ as plotted in Fig. 6 was not constant.

It increased from 0.2 at 1.67 rev/s to 0.5 at 10 rev/s. This implies that the influence of shaft speed on heat transfer is stronger than to be expected from the penetration theory. This phenomenon may be accounted for by a gradual transition of the flow type in the SSHE. At low shaft speeds a Couette flow type is likely to occur. This is a simple shear flow in which the radial velocity component is zero outside the area of the scraperblades. If shaft speed increases Taylor vortices gradually start to develop, introducing an extra radial transport (Trommelen 1970; Trommelen and Beek 1971).

Roux. Roux has a firmer consistency than velouté sauce. This results in lower heat transfer coefficients. Figure 7 shows that h_s increases from 670 to 1330 W/m^{2}K with shaft speeds increasing from 1.67 to 8.33 rev/s.

A decrease in h_s with increasing mass flow rates is noticed at higher shaft speeds. The reason for this strange and inconsistent phenomenon is

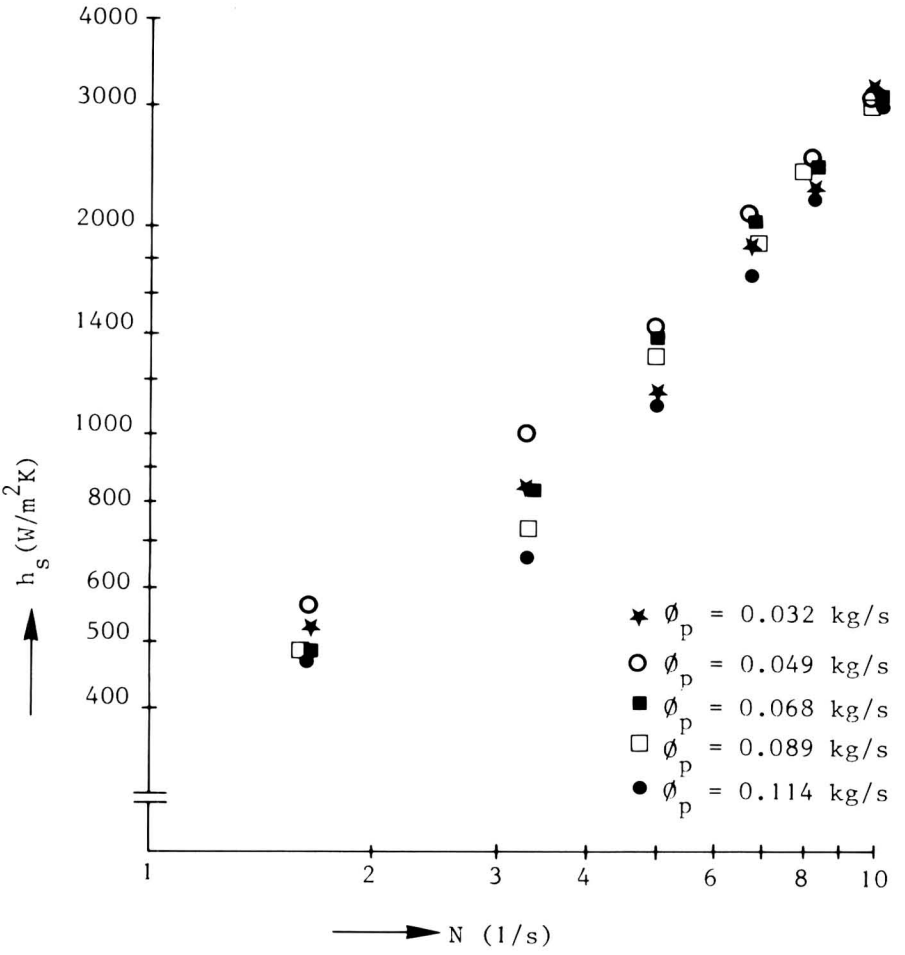

FIG. 5. INFLUENCE OF THE SHAFT SPEED ON THE HEAT TRANSFER COEFFICIENT h_s AT VARIOUS PRODUCTS MASS FLOW RATES
Product: velouté sauce

not clear. With ragout, a quite similar product, this effect did not occur (see Fig. 9, to be discussed later).

The empirical correction factor ϕ fluctuated between 0.2 and 0.3 (see Fig. 8).

The average ϕ-value amounted to 0.24. The factor $N^{0.5}$ in the penetration model is in conformity with the results of the experiments. A Couette-like flow type is most likely to occur for this product. Radial

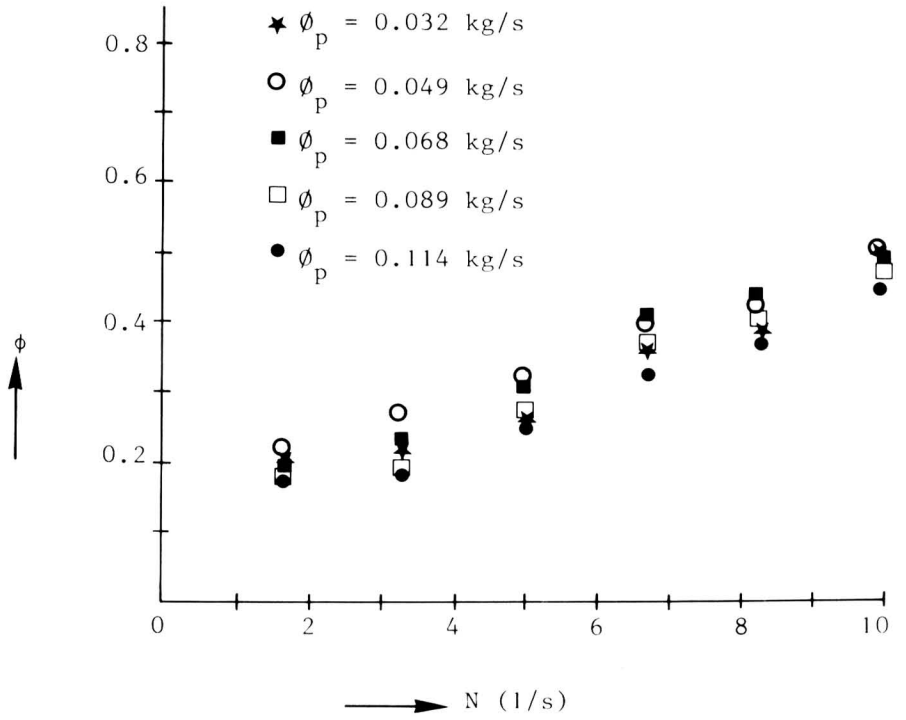

FIG. 6. INFLUENCE OF THE SHAFT SPEED ON THE CORRECTION FACTOR ϕ AT VARIOUS PRODUCT MASS FLOW RATES
Product: velouté sauce

convective heat transport is probably limited, due to suppression of vortex formation. This explains the low values for ϕ.

Ragout. The composition of ragout is almost identical to that of roux. It differs in that it contains 10% meat cut in small pieces. The heat transfer coefficients are summarized in Fig. 9.

The h_s-values show a more pronounced scattering between the different experiments. Values ranged from about 780 W/m^{2}K at 1.67 rev/s to 1900 W/m^{2}K at 8.33 rev/s. Mass flow rate had no consistent effect on the heat transfer. The average ϕ-value is 0.33 and is independent of shaft speed (Fig. 10).

The heat transfer coefficients, being circa 20% higher than in the experiments with roux, must be caused by the presence of the meat, which to some extent presumably disturbs the laminar Couette-flow. However, the depth of the disturbances will be limited in consequence of the small dimensions of the solid pieces.

SUMMARY AND CONCLUSIONS

A method has been worked out for evaluating heat transfer coefficients in the cooling jacket as a function of coolant flow rate. For the SSHE under investigation an empirical relationship for the heat transfer coefficient at the cooling water side is expressed in a dimensionless equation (Eq. 10). Deviations from the generally applied Dittus Boelter formula are small.

For water, heat transfer coefficients at scraped surface increased from 3200 W/m^{2}K at shaft speeds of 1.67 rev/s to 7800 W/m^{2}K at 10 rev/s. The penetration model forms a good basis for the description of the heat transfer in a SSHE. However, for viscous products the model requires

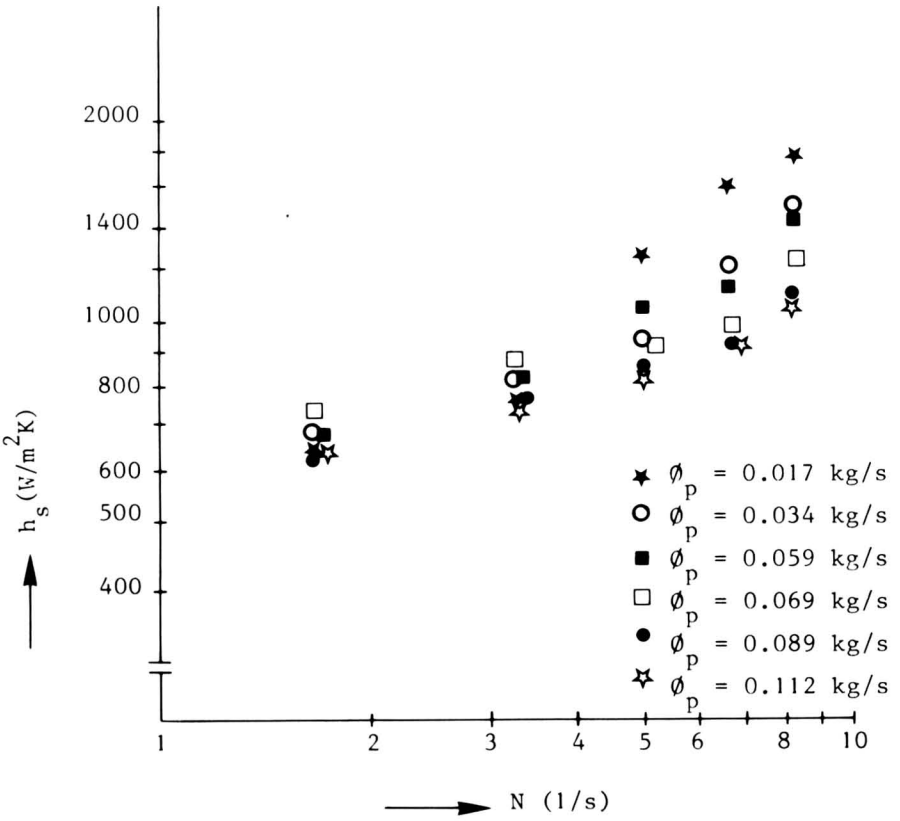

FIG. 7. INFLUENCE OF THE SHAFT SPEED ON THE HEAT TRANSFER COEFFICIENT h_s AT VARIOUS PRODUCT MASS FLOW RATES
Product: roux

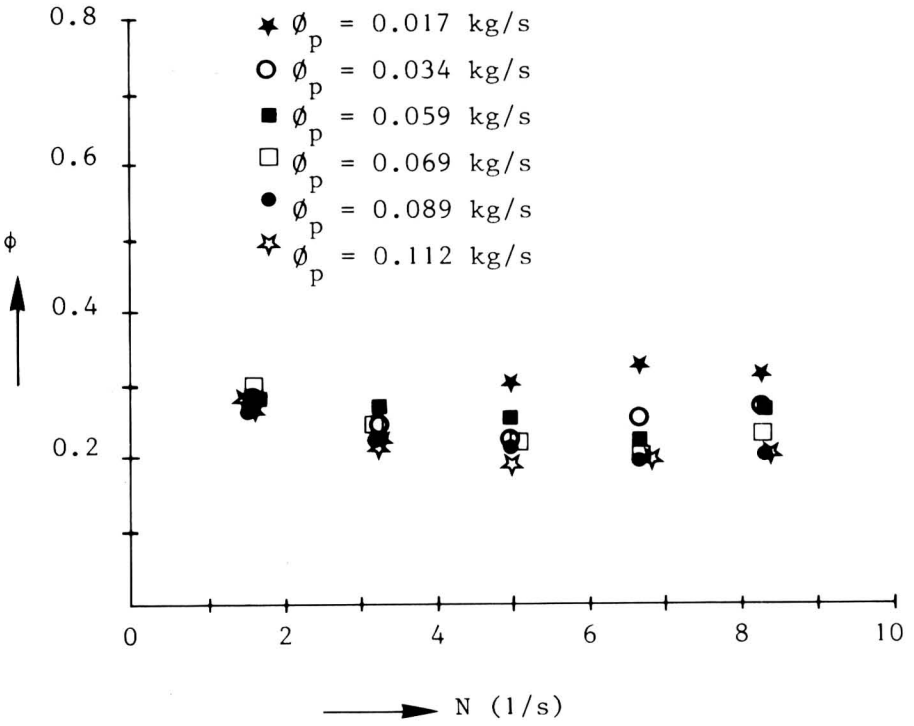

FIG. 8. INFLUENCE OF THE SHAFT SPEED ON THE CORRECTION FACTOR ϕ AT VARIOUS PRODUCTS MASS FLOW RATES
Product: roux

the addition of an empirical correction factor. This especially applies to food products that often show a complicated flowing behavior.

For roux the experimental heat transfer coefficients increased from 670 to 1330 W/m^{2}K with shaft speeds increasing from 1.67 to 8.33 rev/s. With an empirical correction factor of 0.24 the data fitted to the values expected of the penetration theory. Heat transfer coefficients for ragout ranged from 780 to 1900 W/m^{2}K in the explored shaft speed range. The correction factor was independent of shaft speed and mass flow. With $\phi = 0.33$ the results fitted to the penetration model. The presence of the meat had a slightly favourable effect on heat transfer. With respect to the velouté sauce, which has a weaker consistency, the situation was different. Heat transfer coefficients varied from 500 W/m^{2}K at 1.67 rev/s to 3150 W/m^{2}K at 10 rev/s. The correction factor increased in this shaft speed range from 0.20 to 0.50. Presumably, a gradual transition of the flow type had taken place (Couette flow to Taylor vortices). The firm

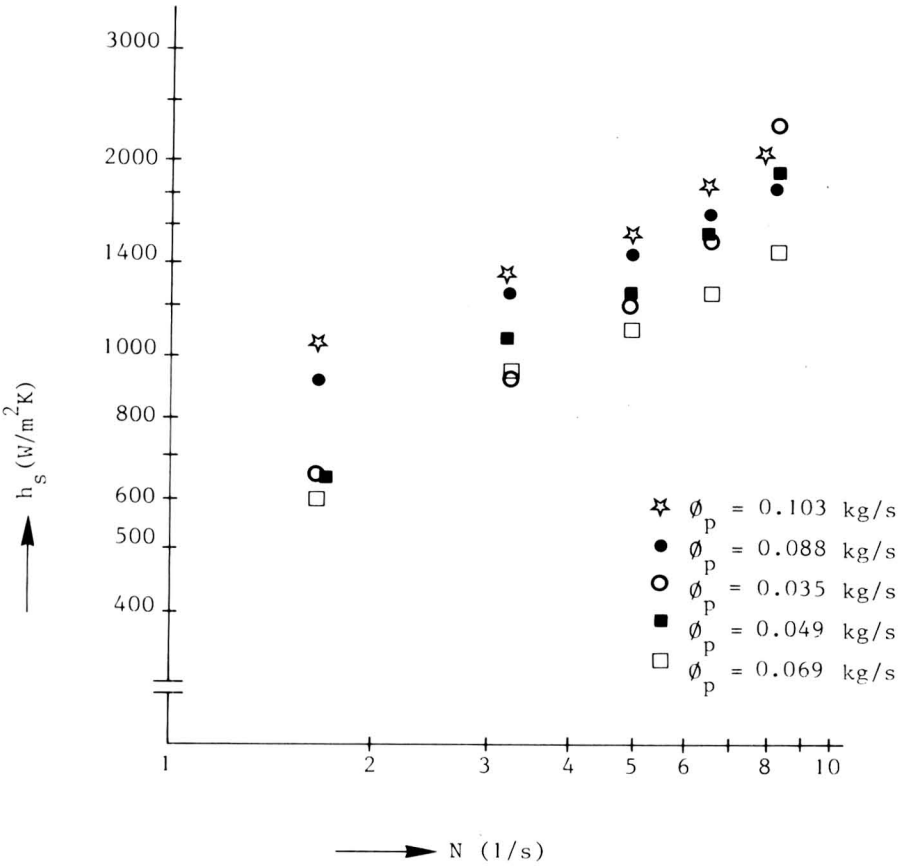

FIG. 9. INFLUENCE OF THE SHAFT SPEED ON THE HEAT TRANSFER COEFFICIENT h_s AT VARIOUS PRODUCT MASS FLOW RATES
Product: ragout

shear forces in the SSHE resulted in a change in structure for the products roux and ragout. After passing the SSHE a beginning fat separation was observed.

In the literature various data are to be found concerning heat transfer to newtonian fluids in a SSHE. However, there is little information available on heat transfer to highly viscous non-newtonian fluid products. This study has supplied data on heat transfer to some food products with a rather firm consistency which will prove to be useful for designing and engineering purposes.

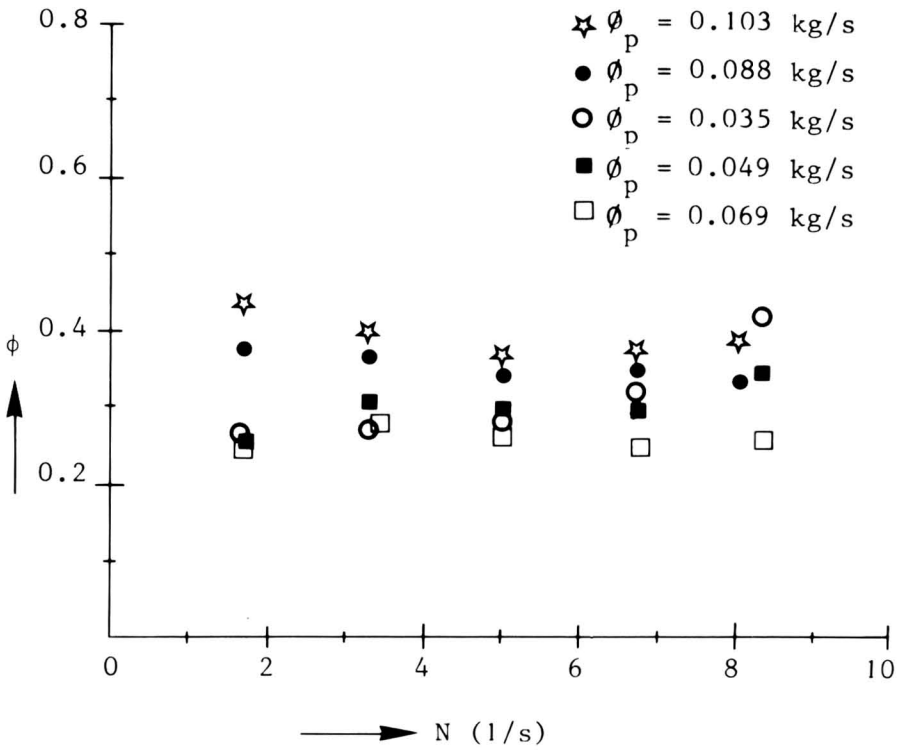

FIG. 10. INFLUENCE OF THE SHAFT SPEED ON THE CORRECTION FACTOR ϕ AT VARIOUS PRODUCT MASS FLOW RATES
Product: ragout

NOMENCLATURE

A = logarithmic mean area heat transferring wall, m^2
c_p = specific heat product, J/kg K
d_t = inside diameter product cylinder, m
d_s = shaft diameter, m
d_h = hydraulic diameter, m
h_s = heat transfer coefficient at scraped side, W/m^2K
h_j = heat transfer coefficient in cooling jacket, W/m^2K
k_c = thermal conductivity coolant, W/mK
k_p = thermal conductivity product, W/mK
k_w = thermal conductivity wall material, W/mK
N = shaft speed, 1/s
n = number of rows of scraper blades
Nu = Nusselt-number

Pr = Prandtl-number
q = heat flow, W
Re = $vd_h\rho/\mu$ Reynolds-number
Re_a = $v(d_t - d_s)\rho/\mu$ axial Reynolds number
Re_r = $Nd_t^2\rho/\mu$ rotational Reynolds number
R_e = external radius heat transferring wall, m
R_i = internal radius heat transferring wall, m
$R_{\ln}$ = logarithmic mean radius heat transferring wall, m
ΔT_c = temperature difference inlet and outlet coolant, °C
ΔT_p = temperature difference inlet and outlet product, °C
$\Delta T_{\ln}$ = logarithmic mean temperature difference, °C
U = overall heat transfer coefficient, W/m^2K
v = average flow velocity, m/s
x = thickness heat transferring wall, m
ρ_p = density product, kg/m^3
ρ_c = density coolant, kg/m^3
ϕ = correction factor
μ = viscosity, Ns/m^2
ϕ_c = mass flow rate coolant, kg/s
ϕ_p = mass flow rate product, kg/s

REFERENCES

ANTON, J. D. 1977. The Contherm scraped-surface heat exchange. I.F.S.T. Proceedings, *10*(3), 137–142.

CUEVAS, R. and CHERYAN, M. 1980. Heat transfer to a liquid food system in a scraped-surface heat exchanger. In *Foods Processing Engineering*, Vol. 1 (P. Linko, Y. Mälkki, J. Olkku and J. Larinkari, eds.) pp. 506–510, Applied Sciences Publishers, Ltd., London.

HARRIOTT, P. 1959. Heat transfer in scraped-surface exchangers. Chem. Eng. Prog. Symp. Ser *55*(29), 137–139.

HOULTON, H. G. 1944. Heat transfer in the Votator. Ind. Eng. Chem. *36*, 522–528.

LATINEN, G. A. 1959. Discussion of the paper Correlation of scraped film heat transfer in the Votator. Chem. Eng. Sci. *9*, 263–266.

SKELLAND, A. H. P., OLIVER, D. R. and TOOKE, S. 1962. Heat transfer in a water-cooled scraped-surface heat exchanger. Br. Chem. Eng. *7*, 346–353.

TROMMELEN, A. M. 1967. Heat transfer in a scraped-surface heat exchanger. Trans. Inst. Chem. Eng. (London) *45*, T176–T178.

TROMMELEN, A. M. 1970. Physical aspects of scraped-surface heat exchangers. Thesis, University Delft, The Netherlands.

TROMMELEN, A. M., BEEK, W. J. and WESTELAKEN, H. C. van de 1971. A mechanism for heat transfer in a Votator-type scraped surface heat exchanger. Chem. Eng. Sci. *26*, 1987–2001.

TROMMELEN, A. M. and BEEK, W. J. 1971. Flow phenomena in a scraped-surface heat exchanger (Votator-type). Chem. Eng. Sci. *26*, 1933–1942.

FACTORS AFFECTING PERFORMANCE OF BRINE DRIVEN EVAPORATORS

KONG-HWAN KIM[1], HENRY G. SCHWARTZBERG[2] and JOHN R. ROSENAU

Department of Food Engineering
University of Massachusetts
Amherst, MA 01003

Received for Publication October 15, 1982
Accepted for Publication January 4, 1983

ABSTRACT

Concentrated $CaCl_2$ and LiCl brines were used to evaporatively concentrate liquid foods. The concentration was carried out in double falling film evaporators in which brine flowed down the outside of the tubes and liquid food flowed down the inside. The vapor spaces between the brine and the food were connected and vapor from the food was absorbed in the brine. The heat generated by vapor absorption in the brine provided the heat needed to sustain evaporation, and was transferred to the food because of the boiling point elevation of the brine. Evaporation rates approaching those obtained in commercial evaporators were obtained for skim milk, sugar solutions and orange juice. The evaporation rates were affected by flow rates, temperature, concentration and tube material.

INTRODUCTION

Calcium chloride brines and other hygroscopic brines readily absorb water vapor and therefore in principle can be used to evaporatively concentrate water-containing liquid foods. The brine, which is diluted in this process, can be reconcentrated by solar induced evaporation. Because the concentrated and dilute brines can be stored, the combined use of such evaporators and solar concentrated brines provides a method

---

[1]Present address: Division of Agricultural & Food Engineering, Asian Institute of Technology, G.P.O. Box 2754, Bangkok, Thailand 10501

[2]To whom correspondence should be sent

Journal of Food Process Engineering 7 (1983) 37–62.

whereby solar energy can be used to concentrate foods without synchronization of the food concentration process and periods of sunshine.

The use of concentrated brines for refrigeration has been studied by a number of investigators (Taylor 1929; Thomas and Anderson 1942; Pierce 1945; Berestneff 1950a, 1950b; Friend 1952; Ashley 1954; Ellington *et al.* 1957; Hollands 1963; Malpas 1972; Lof and Thybout 1964; Krieth and Krieder 1978). In 1977 Schwartzberg proposed a brine-driven evaporator for concentrating liquid foods. The proposed idea was put into practice by Schwartzberg and Rosenau (1979). Evaporative concentration and freezing techniques were developed in conjunction with solar collection and brine reconcentration methods (Schwartzberg *et al.* 1980).

The objectives of this study were: (1) to determine the technical feasibility of the brine induced evaporation system; and (2) to evaluate the rate and energy factors involved in its operation.

EXPERIMENTAL

Choice of Brine

Various hygroscopic salts such as LiBr, LiCl, $MgCl_2$, and $CaCl_2$ can be used in brine induced evaporation systems. The choice between these salts depends on their cost and the ΔT, solubility, and water absorption capacity they provide for processing use. To be feasible, the brine must be inexpensive. While LiCl and LiBr provide higher ΔTs, the high cost of these brines initially appeared to preclude their use for the brine induced evaporation, particularly when long-term storage of large amounts of brine is necessary. $CaCl_2$ is low cost, readily available, nontoxic in relatively large doses, and can provide fairly high ΔTs. In addition, the solubility of $CaCl_2$ is higher than that of $MgCl_2$. Due to these advantages over the other brines mentioned above, $CaCl_2$ was chosen to be used in this work.

Choice of Liquid Food

To clearly identify brine use dependent operating characteristics a major portion of the experiment was carried out with tap water, which completely eliminated food solute-induced problems. Additional feasibility demonstration tests were carried out using sugar solutions and orange juice.

Equipment

The liquid foods were concentrated in a brine-induced evaporator which consisted of a vertical tube wetted-wall column, two reservoirs, and various attachments for controlling and measuring operation conditions (Fig. 1).

The vertical annular column was formed by a 1.212 m length of 0.0254 m O.D. stainless steel tube placed concentrically inside a 0.0762 m O.D. stainless steel tube. The entering liquid food was introduced at the top of the evaporator and was put in film flow inside the 0.0254 m tube by a liquid food distribution weir. As the film of liquid food was heated in its downward flow by the preheated brine flowing down the outside of the 0.0254 m tube, vapor evaporated from the film surface and flowed down the center of the tube. The vapors were transferred through a line from the head space of the liquid food reservoir, to the evaporator shell and were absorbed by the brine. Two single-stage centrifugal pumps were used to recirculate the liquid food and the brine. Short-stem mercury thermometers were used to measure the temperatures of both brine and liquid food. Two previously calibrated flow meters ensured constant feed rates to the top of the evaporator throughout the run. The vapor spaces were connected to a vacuum pump, capable of preventing the accumulation of noncondensibles.

Tests were carried out in a similar glass evaporator which was used to observe the internal liquid flow distribution and verify operational feasibility before constructing the stainless steel unit.

Procedure

The following test procedure was used. The brine and liquid food reservoirs were filled and brine circulation was started. The brine passed through a preheater where it was heated to its anticipated operating temperature (i.e., the brine's boiling point elevation plus the boiling point of water at the selected operating pressure). The liquid food was then recirculated and heated by heat transfer from the brine across the evaporator tube. When the desired liquid food temperature was reached, the vacuum pump was started and the system was quickly brought down to the desired operating pressure which was controlled within ± 1.5 mm Hg by means of a mercury-filled cartesian manostat. Manometer and barometer readings were taken to determine the absolute pressure in the system. The brine and food inlet and outlet temperatures and the levels in the cal-

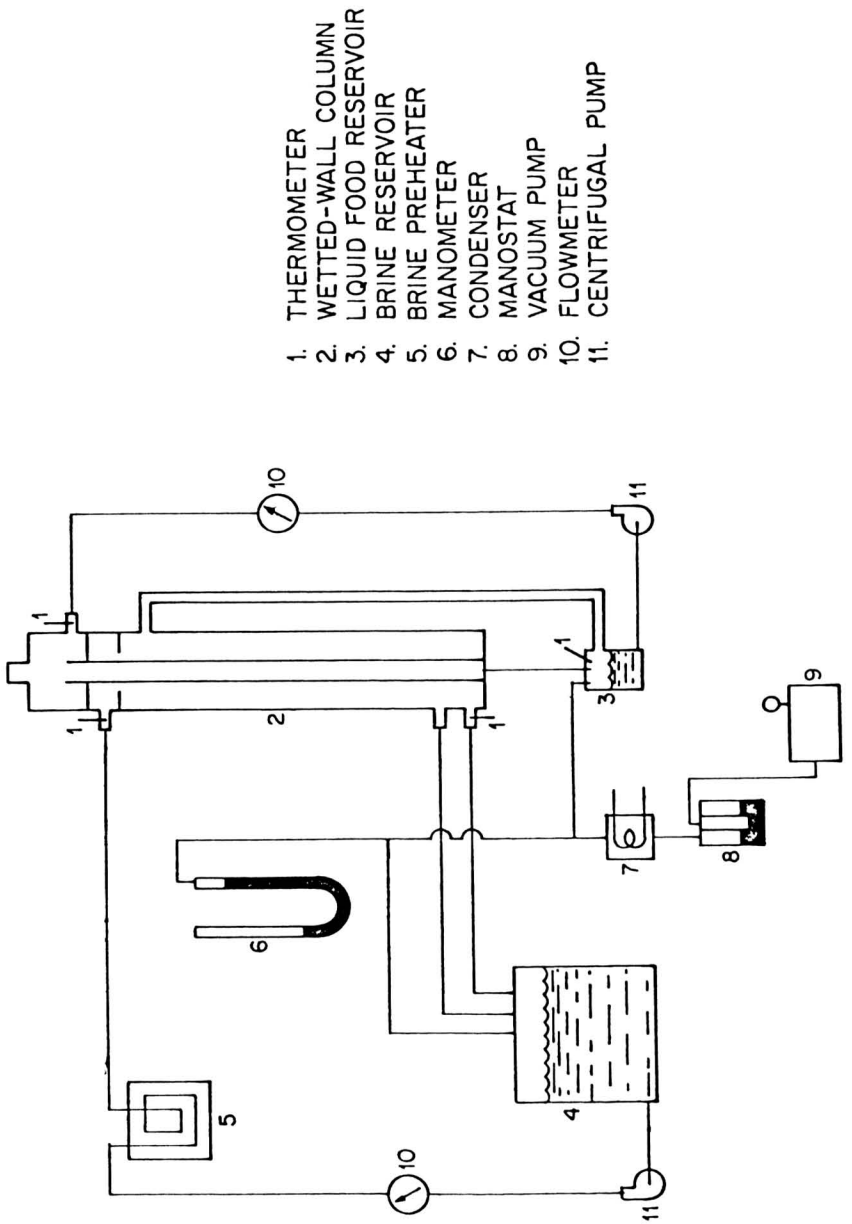

FIG. 1. SCHEMATIC DIAGRAM OF A BRINE INDUCED EVAPORATION SYSTEM

ibrated brine and food reservoirs were periodically read to determine evaporation temperatures, heat-transfer ΔTs, and evporation rates. Liquid food samples were periodically withdrawn by a hypodermic needle inserted through a rubber sampling diaphragm in the discharge line of the liquid food recirculation pump and their concentrations were measured by a refractometer. A sufficient volume of brine was used so that its concentration did not change excessively during a run. Table 1 lists the experimental variables studied.

Performance of the Brine Driven Evaporator

An extensive series of $CaCl_2$ brine driven evaporation tests were successfully performed using both the glass tube and the stainless steel unit to concentrate various aqueous food and food simulant solutions. For most tests, the liquid food temperatures were maintained nearly constant (e.g., 45°C ± 1°C) during the test but the brine temperatures progressively dropped 2–4°C. The ΔT available for heat transfer dropped 3–5°C during the 1–3 h runs. As evaporation proceeded, the brine became more dilute (e.g., the $CaCl_2$ concentration decreased from 41% to 39%) and its boiling point elevation decreased even though a large excess of brine was used to maintain a nearly constant concentration. In most of the evaporator tests, virtually all the water vapor evaporated from the liquid food was absorbed in the brine and very little vapor (e.g., less than 0.5%) was collected in the condenser and dessicant ($CaSO_4$)

Table 1. Ranges of experimental variables

Variable	Range
Brine	$CaCl_2$, LiCl
Liquid food	Water, sugar solution Skim milk, orange juice
Water flow rate	27.0, 61.0, 75.2, 98.2 dm^3/h
Sugar solution flow rate	40.5, 62.7, 92.9 dm^3/h
$CaCl_2$ flow rate	118.2, 205.3, 262.1, 359.7 dm^3/h
$CaCl_2$ concentration	20, 30, 40%
Sugar concentration	10, 20, 30%
Orange juice concentration	5.6, 11.4%
Water temperature	45, 53, 60°C
Sugar temperature	45, 53, 60°C
Tube material	Glass, stainless steel

traps in the vacuum line. The results obtained in the evporation tests using the stainless steel unit are given in Table 2.

Effect of Flow Rates

The evaporation rate increased when the brine flow rate increased. This apparently occurred because high brine flow rates tend to reduce the mass-transfer resistance at the brine surface, thereby minimizing polarization, i.e., excess surface dilution of the brine. Since the surface concentration of the brine determines the boiling point elevation driving the evaporation process, polarization reduces ΔT and the evaporation rate. As shown in Fig. 2, the ΔT tends to more closely approach the theoretical value of 15.1 °C as the brine flow rate increases. The fact that a ΔT of 15.1 °C was never achieved even at the highest brine flow rate indicates that residual polarization still exists. However, part of the discrepancy between the observed and the theoretical ΔT may be due to the presence of noncondensibles and partly may be due to the use of bulk stream temperature measurements rather than surface temperatures, which will be discussed later. There may be two opposing effects with respect to brine flow rate: increased surface waviness provided a high surface mixing rate, which minimizes polarization, but also increased film thickness which, despite the increased waviness, may cause an increased heat transfer resistance.

It can be seen that the evaporation rate increased as the liquid food flow rate decreased. This apparently was due to a reduction in the thickness of the liquid food film thereby facilitating heat transfer across that film. Both water and 20% sugar solutions were used for such tests and each showed a similar trend (see Fig. 3 and 4). The increased vapor flow rate associated with the improved heat transfer at low liquid food flow rates may have caused additional drag-induced thinning of the liquid food film, thereby augmenting the increase in heat transfer. It is claimed that such vapor drag effects materially improve heat transfer in the long-tube TASTE falling-film evporators used in the citrus industry.

The vapor flow drag effect would tend to produce a more linear velocity profile in the falling film of liquid food. The difference between the surface temperature and the bulk average temperature would tend to increase as the linearity of the velocity profile increases. It should be noted that control of the temperatures in the system was based on the bulk average food temperature rather than on the surface temperature, which was not known. Since this surface temperature was lower than the bulk average temperature, this mode of control could have been condu-

Table 2. Summary of results for stainless steel unit

Run	$CaCl_2$ Concentration (%)	Liquid Food	Liquid Food Concentration (%)	$\dot{v}_B$ (dm^3/hr)	$\dot{v}_L$ (dm^3/hr)	T_{Bi} (^oC)	T_{Bo} (^oC)	T_{Li} (^oC)	T_{Lo} (^oC)	ΔT (^oC)	P_{ab} (mmHg)	$\dot{W}$ (kg/hr)	U ($W/m^2 \cdot K$)
1	40.6-38.2	Water	-	262.14	27.0	57.0	57.0	42.5	44.8	13.3	69.8	1.502	847
2	40.9-38.5	Water	-	262.14	60.96	55.4	56.1	44.0	44.9	11.3	71.0	1.363	906
3	41.1-39.4	Water	-	262.14	75.18	55.4	54.4	43.9	45.0	10.5	70.7	1.323	972
4	40.6-38.8	Water	-	262.14	98.22	55.2	54.9	44.9	45.9	9.7	72.6	1.252	1039
5	40.8-39.5	Water	-	118.17	60.96	54.8	54.7	44.4	45.3	9.9	71.8	1.159	892
6	40.5-38.4	Water	-	205.25	60.96	56.0	56.4	45.0	45.8	10.8	73.0	1.306.	903
7	41.0-39.7	Water	-	359.67	60.96	56.5	56.6	44.3	45.4	11.7	70.9	1.470	986
8	40.9-39.1	Sugar	18.6-29.8	262.14	40.52	57.3	57.2	44.2	46.0	12.2	72.5	1.309	819
9	40.5-39.1	Sugar	18.9-30.3	262.14	62.71	56.8	56.6	44.5	46.1	11.4	73.6.	1.227	864
10	40.6-39.3	Sugar	19.9-27.5	262.14	92.90	55.8	55.7	44.7	46.2	10.3	72.6	1.109	922
11	40.8-38.9	Sugar	9.4-16.3	262.14	59.95	55.8	55.6	44.5	45.9	10.5	73.8	1.256	947
12	41.0-39.6	Sugar	29.7-39.0	262.14	65.68	55.4	55.4	45.1	46.2	9.8	73.6	.948	769
13	31.3-30.7	Water	-	241.92	60.96	51.5	51.2	43.6	45.6	6.7	74.7	1.012	1300
14	40.9-38.9	Orange Juice	5.5-9.0	262.14	58.34	56.5	55.9	43.5	45.7	11.6	73.4	1.309	981
15	40.6-39.0	Orange Juice	11.1-17.3	262.14	60.28	56.5	56.1	43.4	45.6	11.8	72.2	1.230	972
16	40.9-39.1	Sugar	28.4-43.8	262.14	65.68	71.9	71.2	59.2	61.1	11.4	149.5	1.291	881
17	40.8-39.5	Sugar	27.3-41.3	262.14	65.68	64.3	63.5	52.9	54.1	10.4	108.0	1.148	850
18	41.0-39.2	Water	-	262.14	60.96	62.5	61.5	51.3	53.0	9.9	105.6	1.352	1075
19	40.8-38.9	Water	-	262.14	60.96	68.7	67.6	57.8	59.9	9.3	148.4	1.323	1142
20*	40.7-38.7	Water	-	233.62	60.96	58.8	59.0	44.3	45.9	13.7	73.3	1.889	1061
21*	41.0-38.8	Sugar	29.3-44.6	233.62	65.68	58.0	57.7	45.5	47.1	11.5	76.7	1.230	861

*LiCl was used for run 20 and 21

$\dot{v}_B$ = Brine flow rate

$\dot{v}_L$ = Liquid food flow rate

T_{Bi}, T_{Bo} = Inlet, outlet brine temperature

T_{Li}, T_{Lo} = Inlet, outlet liquid food temperature

ΔT = Average temperature difference

p_{ab} = Absolute pressure

$\dot{W}$ = Evaporation rate

U = Overall heat transfer coefficient

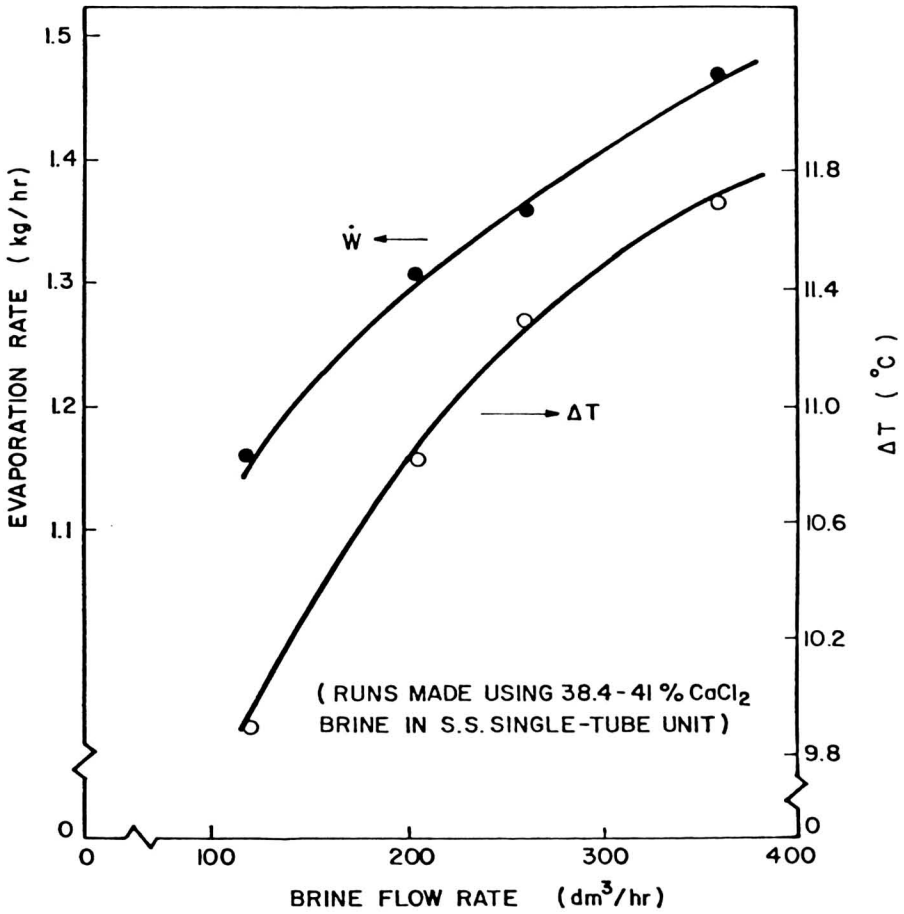

FIG. 2. EFFECT OF BRINE FLOW RATE ON PURE WATER EVAPORATION RATE AND OVERALL ΔT

cive to the accumulation of noncondensibles in the system. Thus the use of higher liquid food flow rates, which would cause a greater difference between the bulk food temperature and the surface temperature, could have indirectly caused an increased accumulation on noncondensibles in the evaporator which, in turn, could have contributed to the reduced evaporation rates experienced at high liquid food flow rates.

Interestingly enough, the evaporation rate and ΔTs fell off in roughly similar proportions as the water flow rate increased, as shown in Fig. 3. The apparent decrease in ΔT may be caused by the fact that the ΔT was based on bulk mixed temperature measurements rather than the true ΔT between the brine surface and the liquid food surface. As the liquid food

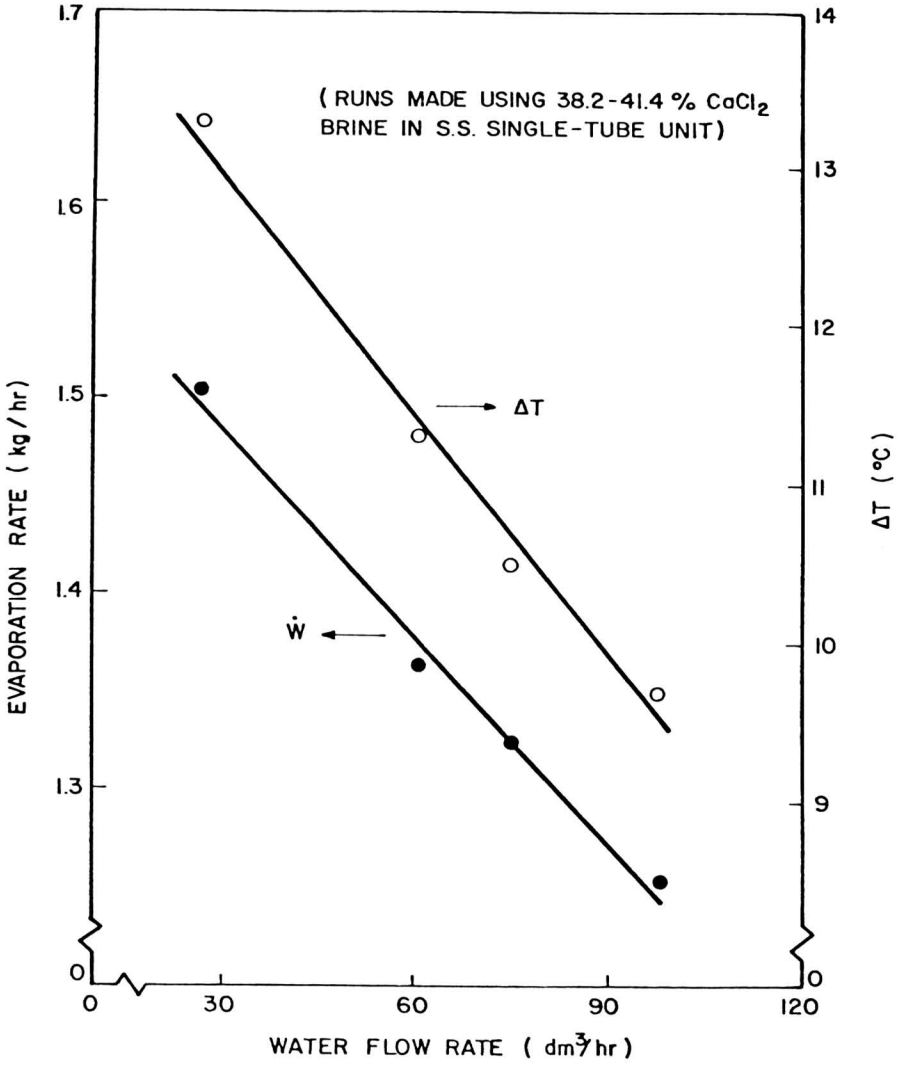

FIG. 3. EFFECT OF WATER FLOW RATE ON PURE WATER EVAPORATION RATE AND OVERALL ΔT

film becomes thicker the temperature drop across that film will increase and as a consequence the mixed bulk liquid food temperature will increase relative to the food surface temperature. This will result in a reduction in the apparent ΔT. A similar reduction in apparent ΔT with increased liquid food flow rates was observed in the case of sugar solution evaporation.

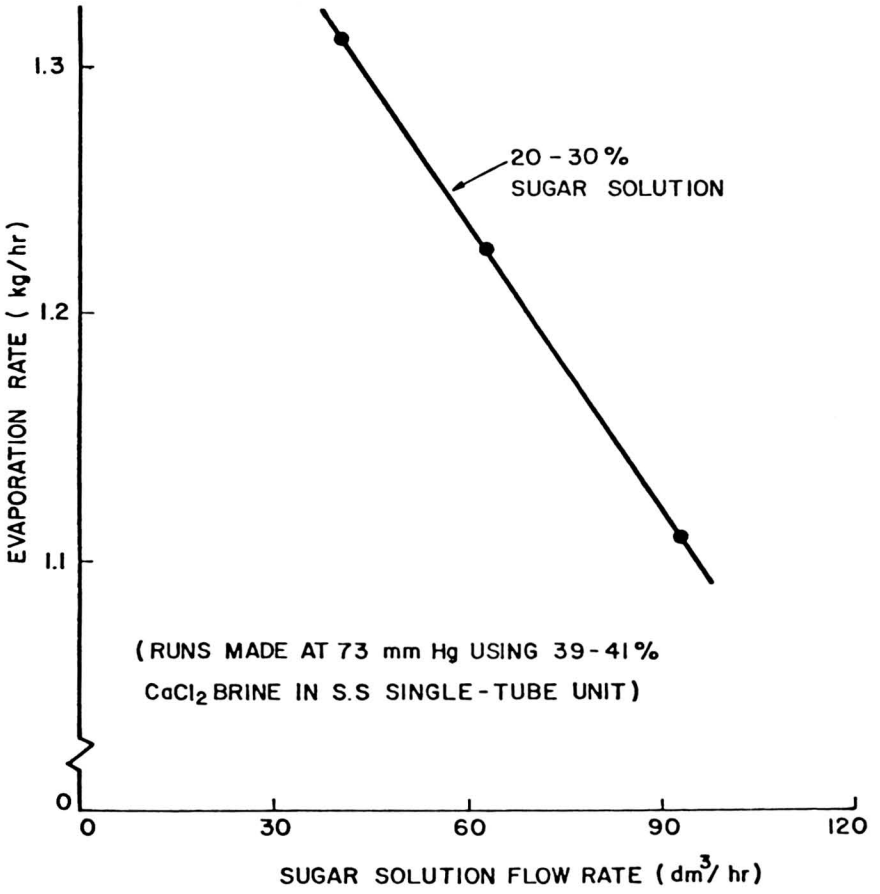

FIG. 4. EVAPORATION RATES VS SUGAR SOLUTION FLOW RATES

Effect of Liquid Food Concentration

For sugar solutions, the evaporation rate progressively decreased as the concentration increased (see Table 3). For the sugar evaporation tests which were carried out in the glass evaporator, where the heat transfer resistance of the glass tube dominated the overall heat transfer resistance, the reductions were mostly due to the progressive reduction in ΔT as the sugar concentration increased. The decrease in ΔT as the sugar concentration increased exceeded the accompanying increase in sugar boiling point elevation. This was probably caused by evaporation induced concentration polarization in the sugar film. Such polarization could produce very rich sugar concentrations at the evaporation inter-

Table 3. Effect of sugar concentration on evaporation rates

Sugar Concentration (%)	Glass Unit		S.S. Unit	
	Evaporation Rate (kg/h)	ΔT (°C)	Evaporation Rate (kg/h)	ΔT (°C)
10–15	0.520	12.1	1.256	11.4
18–29	0.393	9.7	1.227	11.4
30–39	0.279	7.3	0.948	9.8

face. Since the diffusivity of water in sugar solutions decreases markedly as sugar concentration increases, such polarization may tend to be self-enhancing.

The orange juice concentration tests were carried out using the stainless steel unit. The evaporation rates in concentrating 5.5% orange juice to 9.0% were 96% as large as in the water evaporation tests; the rates in concentrating 11.1% orange juice to 17.3% were 90% as large as in the water evaporation tests. (It was found that the concentration levels of orange juice as measured by oven drying were equal to the Brix reading as measured by a refractometer with reasonably good accuracy, i.e., the maximum relative deviation was less than 5%.)

The overall heat transfer coefficients obtained with sugar solutions in the stainless steel evaporator are plotted versus the mean concentration in Fig. 5. The reduction of the overall heat transfer coefficients as the concentration increases probably indicates that the viscosity changes due to concentration changes affect the liquid food-side heat transfer coefficients to some degree.

Effect of Temperature

With sugar solutions there were definite increases in the evaporation rate and heat transfer coefficient as the liquid food temperature increased (see Fig. 6 and 7). Since a reduction in viscosity (from 2.1 to 1.5 cp), as produced by a temperature increase (from 45 to 60°C), will cause a reduction in film thickness, reduced film thickness may account for the behavior shown in Fig. 6. The boiling point elevation of the brine also tends to increase slightly as the evaporation temperature increases and this should cause a slight increase in ΔT and the evaporation rate. As

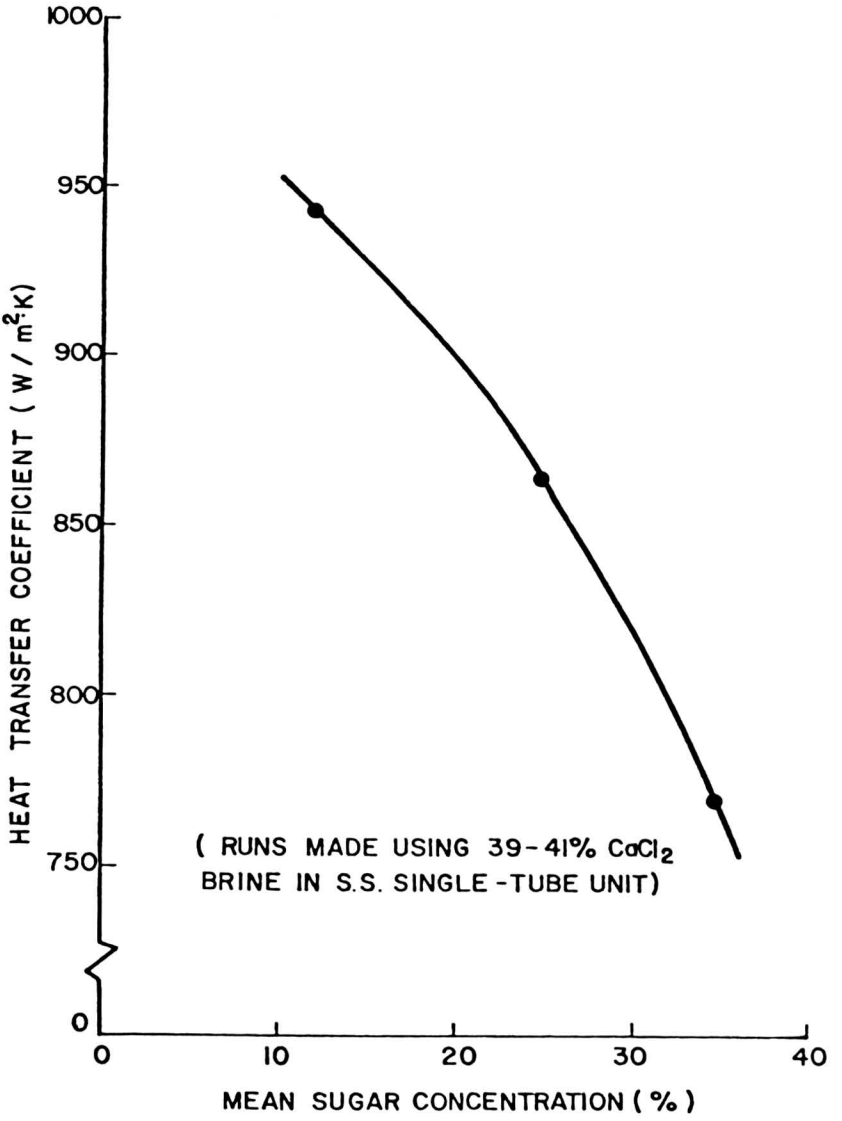

FIG. 5. HEAT TRANSFER COEFFICIENTS VS SUGAR CONCENTRATION

shown in the case of the variation in viscosity with the concentration levels, temperature-induced viscosity changes in liquid food also played an important role affecting heat transfer. The changes in heat transfer coefficients, as shown in Fig. 5 and 7, are also in part attributable to concentration and temperature induced thermal conductivity changes (see

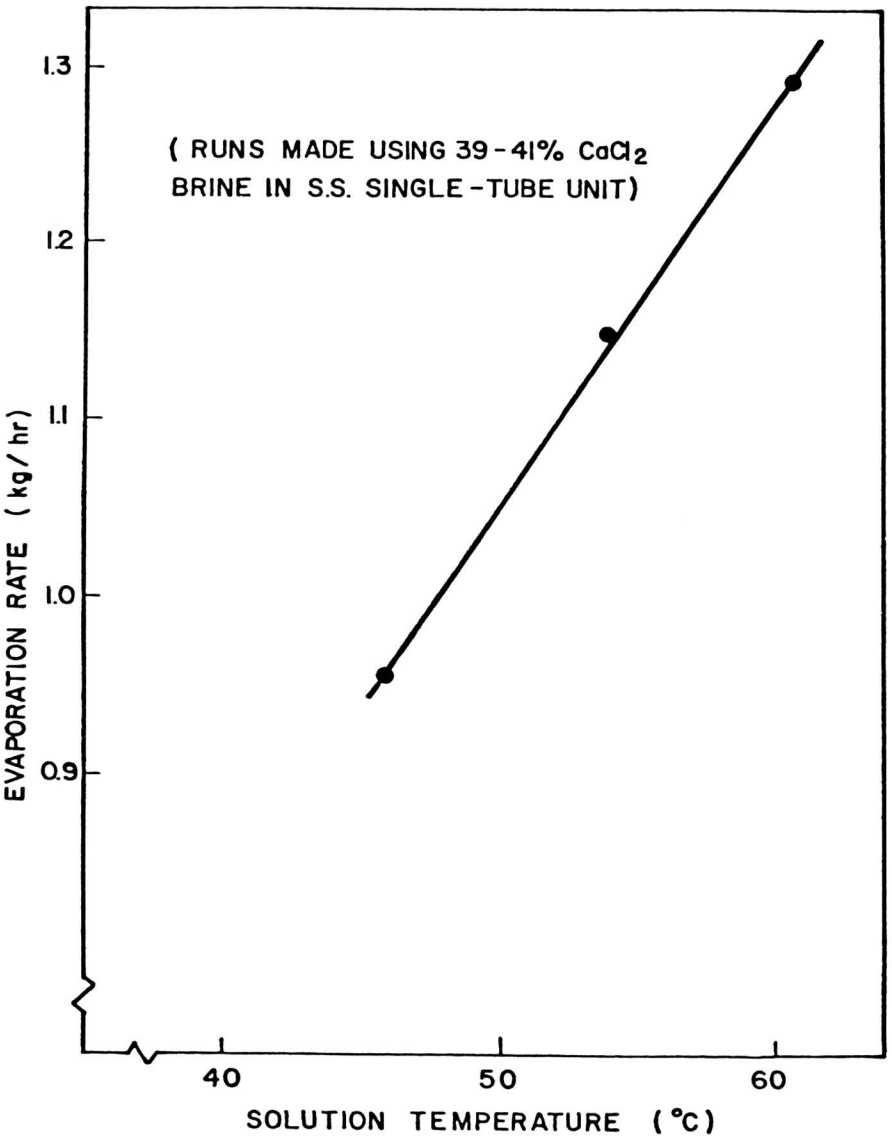

FIG. 6. EVAPORATION RATES FOR 30–40% SUGAR SOLUTIONS VS SOLUTION TEMPERATURE

Table 4); the heat transfer coefficient is roughly proportional to the thermal conductivity.

To determine whether viscosity changes in the brine solution exerted a similar effect on heat transfer, the experiments summarized by Table 5

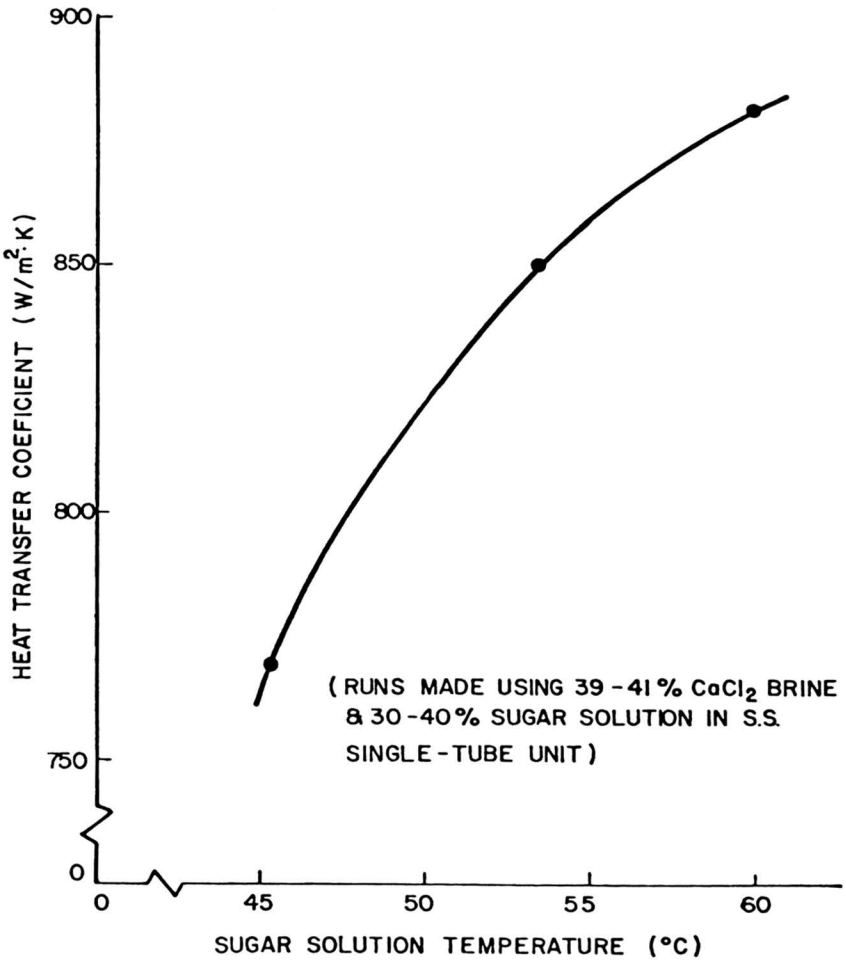

FIG. 7. HEAT TRANSFER COEFFICIENTS VS SUGAR SOLUTION TEMPERATURE

were performed. Since water viscosity changed less markedly than the viscosity of sugar solutions for the temperature ranges used, tap water was used as the evaporated liquid. The results indicate that viscosity changes in brine solution apparently did not affect heat transfer as much as viscosity changes in sugar solution.

Effect of Brine Concentration

Various concentrations of $CaCl_2$ were used to determine their effect on the evaporation rate. As expected, the evaporation rates decreased with

Table 4. Concentration and temperature induced thermal conductivity changes in sugar solutions*

At 50°C,

Concentration of Sugar Solution (%)	Thermal Conductivity (W/m-°K)
10.1	0.601
20.0	0.571
30.0	0.538
30.9	0.502

For 30% sugar solution,

Temperature of Sugar Solution (°C)	Thermal Conductivity (W/m-°K)
1.5	0.478
20.0	0.505
50.0	0.538
80.0	0.504

*From Woodams, E. and Nowrey, J. Food Technology *22*(4), 150–158 (1968).

Table 5. Evaporation rates under the various brine temperatures in s.s. evaporator

40% $CaCl_2$ Temperature (°C)	Evaporation Rate (kg/h)	ΔT (°C)	U (W/m^2·K)
55.8	1.363	11.4	906
62.0	1.352	9.9	1075
68.1	1.323	9.3	1142

Brine flow rate = 262 dm^3/h
Water flow rate = 61 dm^3/h

decreases in the brine concentration due to the lower boiling point elevation (ΔT_{BPE}) obtained at low concentrations. This resulted in smaller ΔT_{EXP} (see Table 6). The ΔT values measured in the evaporation tests ranged from 62% to 78% as large as predicted on the basis of boiling point elevation.

The boiling point elevation of $CaCl_2$ at certain concentrations can be calculated by the following procedure as shown in Fig. 8. A horizontal line is drawn from the ordinate value (operating pressure in mm Hg) to

Table 6. Effect of brine concentration

Evaporator Unit	$CaCl_2$ Concentration (%)	Evaporation Rate (kg/h)	ΔT_{EXP} (°C)	ΔT_{BPE} (°C)	$\Delta T_{EXP}/\Delta T_{BPE} \times 100$ (%)
Glass	20	0.093	3.3	4.4	75
	30	0.364	6.7	8.8	76
	40	0.640	14.3	18.3	78
Stainless steel	30	1.012	6.7	8.8	76
	40	1.363	11.3	18.3	62

ΔT_{EXP} = Temperature difference obtained by experiment
ΔT_{BPE} = Temperature difference based on BPE of brine

the $CaCl_2$ concentration lines. Two reciprocal boiling temperatures are read—one at the concentration of $CaCl_2$ being used and the other at 0% $CaCl_2$. The difference between the reciprocals of these two $1/T$ points is the B.P.E.

The overall ΔT which drives evaporation is the temperature difference between the free surface of the brine and the free surface of the liquid food. Since, as previously pointed out, the observed ΔTs were based on bulk feed and discharge temperatures, part of the ΔT discrepancy may be due to the difference between the corresponding bulk and surface temperatures. Despite the continuous removal of noncondensibles by the vacuum pump, a certain amount of noncondensibles no doubt remained in the evaporator and are partly responsible for lowering the ΔT. The noncondensibles collect in the vicinity of the brine surface and the water vapor must diffuse through these noncondensibles to reach the brine film. The introduction of this diffusion resistance into the vapor path can decrease the rate of condensation far below that for a pure vapor. For example, as little as 1 or 2% of noncondensibles in a system may reduce the rate of heat transfer by 75 to 80% (Foust *et al.* 1959). Noncondensible accumulation reduces the vapor pressure at the brine surface and consequently reduces the brine surface temperature. Vapor flow induced pressure drop between the liquid food reservoir and the brine reservoir may conceivably also cause part of the ΔT discrepancy since the vapor pressure over the brine must be at least slightly lower than the vapor pressure over the liquid food in order to sustain vapor flow. This pressure drop will be discussed further later.

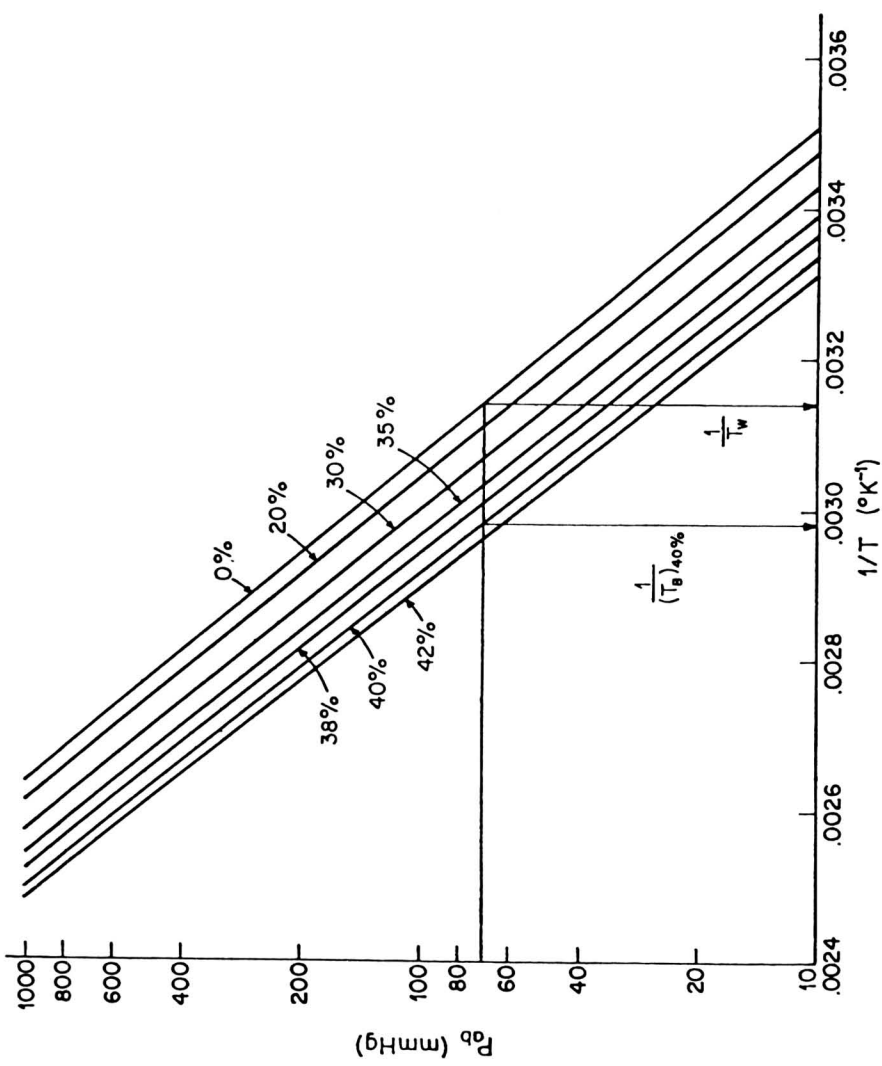

FIG. 8. BOILING TEMPERATURES OF CALCIUM CHLORIDE SOLUTION UNDER VARIOUS PRESSURES

Comparison of the Stainless Steel Evaporator with the Glass Evaporator

When the performance of glass evaporator is compared with that of the stainless steel unit (see Table 7), it can be seen that evaporation was much faster with stainless steel unit. This occurred mainly because of the considerably higher thermal conductivity of stainless steel, 13.85 W/m.K, as opposed to that of glass, 1.08 W/m.K. Since the resistance of the glass tube controlled heat transfer, the brine and liquid food flow rates scarcely affected evaporation rates in the glass unit at all. The overall heat transfer coefficients were 2.5 times higher in the stainless steel unit than those in the glass evaporator. Somewhat larger ΔTs were obtained with glass unit than with stainless steel unit, presumably because the amount of polarization decreases as the evaporation rate decreases.

Use of Lithium Chloride

Because of its high cost, the use of lithium chloride brine for brine induced evaporation is not appropriate when large amounts of brine must be stored for long periods of time. Nevertheless, several pure water and sugar solution evaporation experiments were carried out with lithium chloride to compare the evaporator performance when using such brines versus those for calcium chloride. It was found that the evaporation rate with a 40.7% lithium chloride brine was somewhat higher than that with a 40.9% calcium chloride brine because of the higher boiling point elevation of the lithium chloride brine. The cumulative amount

Table 7. Comparison stainless steel evaporator with glass evaporator

Evaporator Material	Evaporation Rate (kg/h)	Overall Heat Transfer Coefficient ($W/m^2 \cdot K$)	Temperature Difference (°C)
Glass (Borosilicate)	0.36	375	13.9
Stainless steel	1.32	972	11.2

Material being evaporated: water
Brine flow rate: 262 dm^3/h
Water flow rate: 61 dm^3/h

of evaporation increased linearly with time for water; with sugar solution, the concentration increased linearly with the time (see Fig. 9 and 10). As shown in Fig. 11, ΔT decreased more rapidly during evaporation when using the 40% lithium chloride solution than with the 40% calcium chloride solution, but this presumably occurred mainly because the higher rate of evaporation with lithium chloride resulted in a more rapid

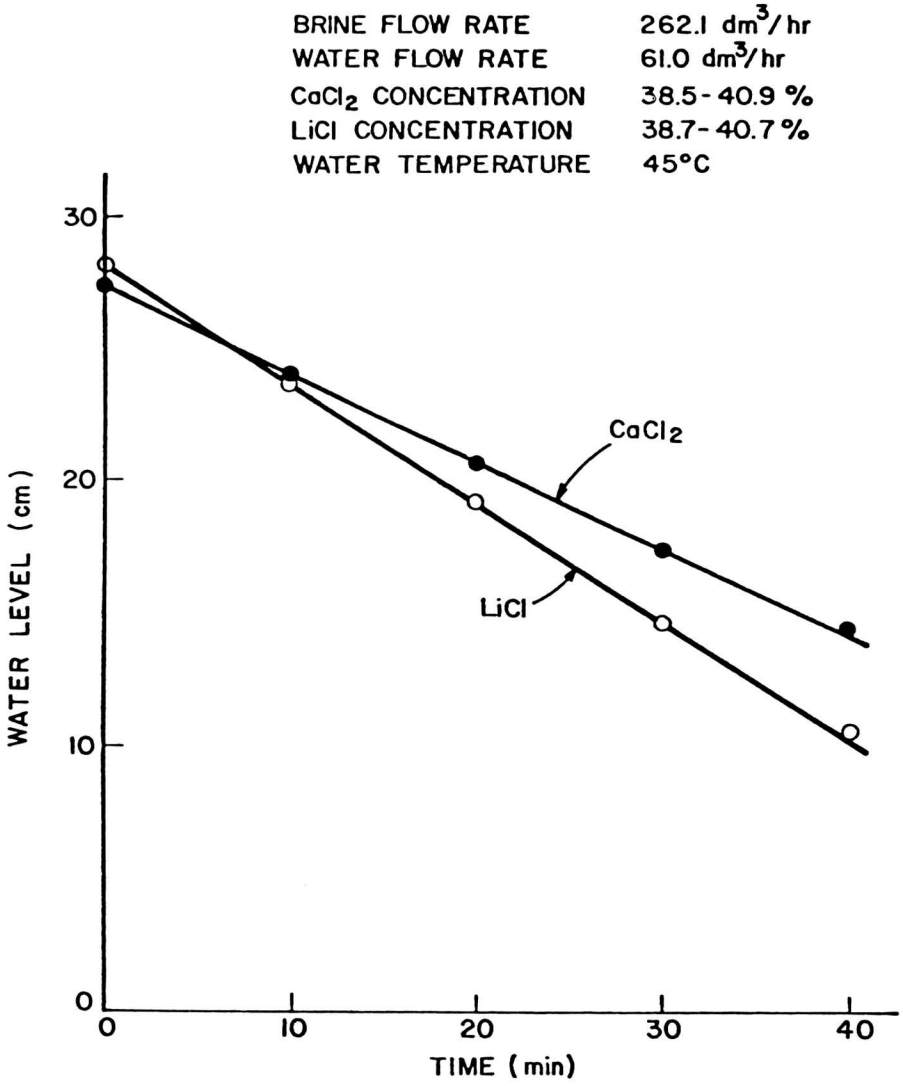

FIG. 9. WATER LEVEL DROP DURING EVAPORATION IN A S.S. EVAPORATOR

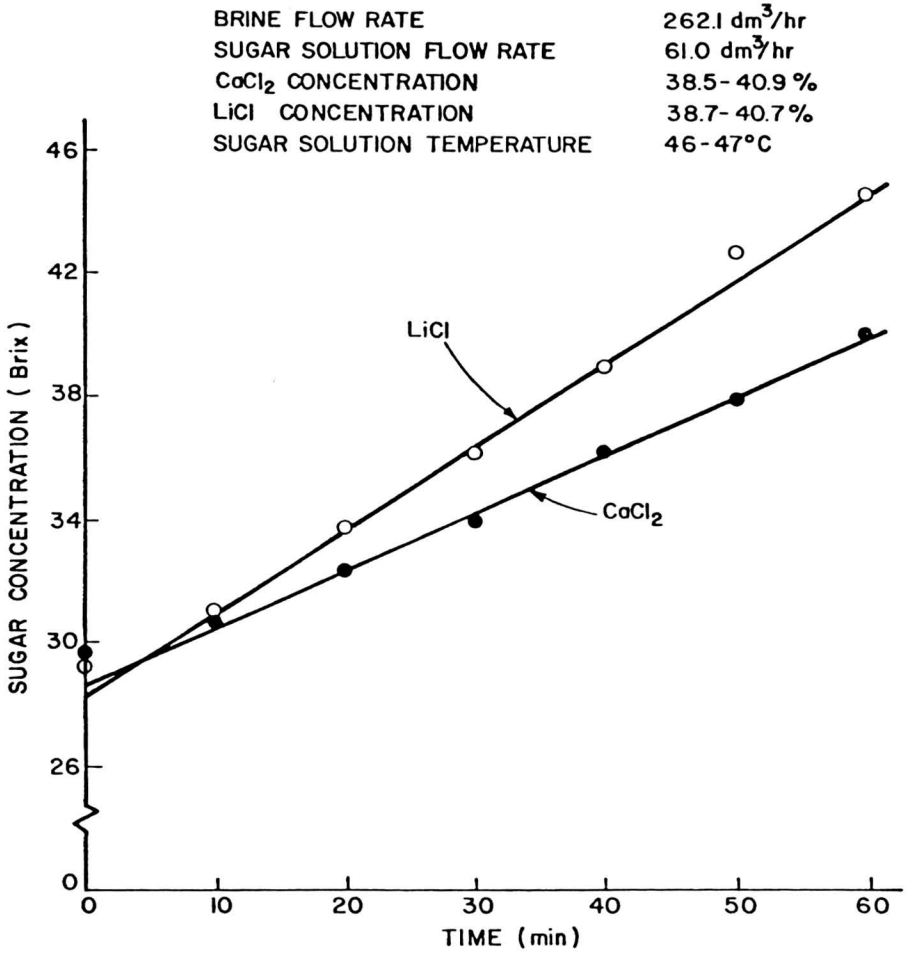

FIG. 10. SUGAR CONCENTRATION CHANGE DURING EVAPORATION IN A S.S. EVAPORATOR

dilution of the brine. A comparison of the overall heat transfer coefficients obtained with lithium chloride brine and calcium chloride brine is presented in Table 8.

Skim Milk Evaporation

Somewhat lower ΔTs and lower evaporation rates relative to pure water were obtained during the skim milk concentration runs in the glass evaporator. The evaporation rates when concentrating 10.5% skim milk

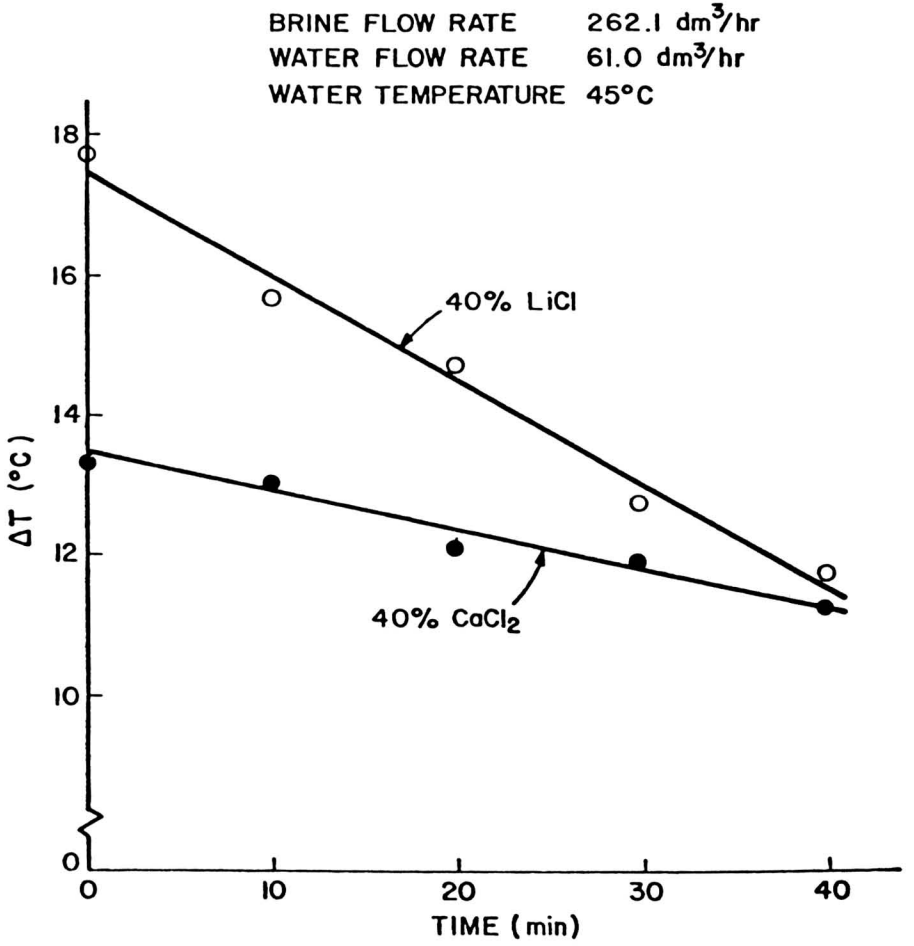

FIG. 11. TEMPERATURE DIFFERENCE CHANGE DURING EVAPORATION IN A S.S. EVAPORATOR

to 16% were only 75% as large as in the dyed water evaporation tests and the ΔT was only 9.4°C as compared to an average of 14°C. Since the fractional reduction in ΔT exceeded the fractional reduction in evaporation rate, the reduction in evaporation rate can't be attributed to impaired heat transfer. Possibly the residual foaming which still persisted after the use of an antifoaming agent somewhat interfered with the vapor transfer process and caused a larger than normal vapor pressure drop between the milk and the brine. Various difficulties were experienced in the skim milk evaporation tests. Excessive foaming, which was initially a problem, was cured by using a food-grade anti-foaming agent.

Table 8. Effect of brine composition on overall heat transfer coefficient

Liquid Food	Overall Heat Transfer Coefficient ($W/m^2 \cdot K$)	
	40% $CaCl_2$	40% LiCl
Water	906	1061
30% sugar solution	769	861

Brine flow rate = 262 dm^3/h
Water flow rate = 61 dm^3/h
Sugar solution flow rate = 66 dm^3/h
Water temperature = 45°C
Sugar solution temperature = 46°C

Bacterial growth and curdling, which was encountered during the long recirculation time (2.5 h) at the 45°C evaporation temperature, is a problem that remains to be overcome. Presumably this problem could be eliminated without causing excessive protein denaturation by operating at temperatures between 60°C and 70°C, and by using long tube single pass evaporation, as is done commercially.

The successful operation of the brine induced evaporator depends upon the water vapor emanating from the liquid food effectively contacting the brine. Thus, there must be a driving force provided by a very slight pressure difference between the brine reservoir and the liquid food reservoir.

The Reynolds number for vapor flow in the vapor transfer line in a typical run in the stainless steel evaporator is 137. Therefore the Poiseuille-Meyer equation for the viscous flow of compressible gases can be used to calculate the pressure drop in the vapor line:

$$\dot{W} = \frac{\pi(P_1^2 - P_2^2)Mg_c d^4}{256RTL\mu}$$

where $\dot{W}$ is the weight rate of water evaporation, P_2 is the pressure of the brine surface, P_1 is the pressure over the water, M is the molecular weight of water, g_c is the mass force conversion constant, d is the diameter of the vapor transfer line, L is the length of that line, μ is the viscosity of water vapor at the evaporation temperature, R is the perfect gas law constant, and T is the absolute temperature.

Rearranging and solving, for P_1,

$$P_1 = \left[P_2^2 + \frac{256 \dot{W} RTL\mu}{\pi M g_c d^4} \right]^{1/2}$$

Substituting 9580.21 N/m^2 for P_2 (i.e., the vapor pressure of water at 45°C), 1.219 m for L, 0.019 m for d, 1.3 kg/h for $\dot{W}$, P_1 is 9602.33 N/m^2. The pressure drop 22.12 N/m^2 is obtained.

Therefore, it can be seen that a very small ΔP is required to drive the water vapor flow. Adequate removal of noncondensibles on the other hand is a much more serious problem. Noncondensibles are introduced into evaporators because of gas dissolved in the liquid fed into the evaporator and because of air leakage at pump seals or other imperfect joints in vacuum evaporators. These noncondensibles are swept by the vapor flow to the condensation surface in a brine induced evaporator. Unless they are removed, they will progressively accumulate at that surface reducing the water vapor pressure and consequently reducing the equilibrium condensation or absorption temperature. For a brine induced system, this temperature reduction in turn reduces the ΔT which drives the evaporation process—thereby greatly reducing the productivity of the evaporator.

The purpose of the vacuum pumping system is to remove these noncondensibles. Ideally the connection to the vacuum system should be made at the most downstream point in the vapor flow path. If not, noncondensibles will be swept to that point and their concentration will rise until it reaches a value which permits the noncondensibles to backdiffuse to the point where the vacuum pumping system is connected to the evaporator. Occasionally the noncondensibles pressure will rise until it equals the total pressure in the system and progressively larger regions of the absorption surface will be blanketed by noncondensibles. This will reduce the evaporation rate and the vapor velocity sweeping the noncondensibles forward until the decreased distance between the blanketed zone and the decreased vapor sweep velocity permits the noncondensibles to diffuse into the vacuum line at a rate which is equal to their rate of entry into the evaporation system. Obviously such conditions result in very marked reductions in evaporation rate.

The importance of proper noncondensible removal was illustrated by two experiments. In one of the experiments a large vacuum connection (4.45×10^{-3} m diameter) was attached to the brine reservoir, the most downstream point in the vapor flow path, and a small vacuum connection (2.54×10^{-3} m in diameter) was attached to the liquid reservoir. In other experiments the small vacuum connection was used at both reservoirs. As shown in Table 9, when the small connection was used at the

Table 9. Effect of pressure difference due to fitting size on evaporation process

Vacuum Outlet Diameter in Brine Reservoir (m)	Overall Temperature Difference (°C)	Evaporation Rate (kg/h)
2.54×10^{-3}	1.37	0.114
4.45×10^{-3}	11.3	1.363

Brine flow rate = 262 dm^3/h
Water flow rate = 61 dm^3/h

brine reservoir the overall ΔT dropped by 88% and the evaporation rate by 92%. These results are further substantiated by runs in which the liquid food temperature was set at a value which provided a vapor pressure higher than the set point for the manostat which controlled the pressure in the evaporator. In these runs the ΔT rose and approached the theoretical ΔT (i.e., the boiling point elevation) closely, but very large amounts of water vapor were collected in the traps in the vacuum line. Under such conditions the vacuum system did more pumping because the manostat control valve, which connects the evaporator to the vacuum system, stayed open and the purging of noncondensibles was very complete. In another experiment where the liquid temperature was set at a value which provided a vapor pressure less than the manostat set pressure, very little if any vapor was trapped in the vacuum line but a marked reduction in the evaporation rate occurred. This problem has its counterpart in the operation of commercial multiple effect evaporators. High rates of noncondensibles removal lead to improved evaporation rates but cause higher steam losses and reductions in energy efficiency. Low rates of noncondensibles removal lead to improved energy efficiency (within limits) but cause reductions in the evaporation rate.

CONCLUSIONS

A double falling film evaporator has been developed to evaporatively concentrate water-containing liquid foods by using hygroscopic brines concentrated by solar energy induced evaporation. Higher evaporation rates (1–1.5 kg/h) were obtained with the stainless steel evaporator as compared to those (0.27–0.37 kg/h) with the glass evaporator. The overall heat transfer coefficients were 2.5 times higher in the stainless steel unit (e.g., 972 $W/m^2.K$) than those in the glass evaporator (e.g., 375

$W/m^2.K$). In stainless steel unit evaporation tests, the evaporation rate increased as the liquid food flow rate decreased and as the brine flow rate increased.

The ΔTs observed were only 62–80% as large as those predicted on the basis of boiling point elevation. This is probably partly due to concentration polarization and incomplete removal of noncondensibles. Part of the apparent ΔT discrepancy may be an artifact due to use of mixed bulk temperatures rather than surface temperatures to calculate the ΔT. The reduction of the overall heat transfer coefficients as the concentration increases and as the temperature decreases indicate that the accompanying viscosity changes affect the liquid food-side heat transfer coefficients.

Despite the continuous removal of noncondensibles by the vacuum pump, some remained in the evaporator and are partly responsible for lowering the ΔT. The noncondensibles collect in the vicinity of the brine surface, and the water vapor must diffuse through these to reach the brine film. The introduction of this diffusion resistance into the vapor path decreases the rate of condensation below that for a pure vapor. The accumulation of noncondensibles reduces the vapor pressure at the brine surface and consequently reduces the brine surface temperature. While $CaCl_2$ brines only provided sufficient boiling point elevation to drive a single effect evaporator, LiCl and LiBr provide boiling point elevations which should be large enough to drive multiple effect evaporators.

ACKNOWLEDGMENT

This research was supported by the Massachusetts Agricultural Experiment Station and the United States Department of Energy (Grant No. 5-28624-20222).

REFERENCES

ASHLEY, C. M. 1954. U.S. Patent No. 2,679,733. Absorption refrigeration system using dilution means. June 1, 1954.

BERESTNEFF, A. A. 1950a. Absorption refrigeration. Mech. Eng. *72,* 216–220.

BERESTNEFF, A. A. 1950b. New absorption refrigeration unit uses water vapor. *Power Generation.* 54, 108, 110, 112, 114, 116, 118.

ELLINGTON, R. T., KUNST, G., PECK, R. E. and REED, J. F. 1957. The absorption cooling process. Inst. Gas Technol. Res. Bul. 14.

FOUST, A. S., WENZEL, L. A., CLUMP, C. W. and ANDERSON, L. B. 1959. *Principles of Unit Operations,* pp. 195, John Wiley & Sons, Inc., New York.

FRIEND, W. F. 1952. Summary of progress made with gas all-year air conditioning. Heating and Ventilating, *49,* 87–90, January.

HOLLANDS, K. G. T. 1963. The regeneration of lithium chloride brine in a solar still. Solar Energy, *7,* 39–43.

KRIETH, F. and KRIEDER, J. 1978. Principles of Solar Engineering. pp. 512, McGraw-Hill, New York.

LOF, O. G. and THYBOUT, R. A. 1974. Design and cost of optimal systems for residential heating and cooling by solar energy. Solar Energy, *16,* 9.

MALPAS, E. W. 1972. Vacuum equipment for evaporative cooling. Process Biochemistry, *7,* 15–17.

PIERCE, H. C. 1945. An all-year gas air conditioning unit. Mech. Eng. *67,* 171–174, 189.

SCHWARTZBERG, H. G. 1977. Energy requirements for liquid food concentration. Food Technology, *31*(3), 67–76.

SCHWARTZBERG, H. G. and ROSENAU, J. R. 1979. Use of solar concentrated water absorbing brines to save energy in food processing. In *Changing Energy Use Futures,* Vol. IV, (R. Fazzolare and C. Smith, eds.) pp. 1922–1931, Pergamon Press, Oxford.

SCHWARTZBERG, H. G., ROSENAU, J. R., KIM, K. H. and YANNIOTIS, S. 1980. The use of solar concentrated brines for food processing. ASAE National Energy Symposium Vol. III. In *Food Processing,* pp. 586–591, Sept. 29–Oct. 1, 1980, Kansas City, Missouri.

TAYLOR, R. S. 1929. Heat operated refrigeration machines of the absorption type. Refrig. Eng. *17,* 136–143, 149.

THOMAS, A. R. and ANDERSON, P. O., JR. 1942. U.S. Patent Nos. 2,282,503 and 2,282,504. Refrigeration. May 12, 1942.

WOODAMS, E. E. and NOWREY, J. E. 1968. Literature values of thermal conductivities of foods. Food Technology, *22*(4), 150–158.

AN APPROXIMATE METHOD FOR DETERMINING THE WASHING TIME AND WATER VOLUME DURING THE BATCH WASHING OF COTTAGE CHEESE CURD

JUAN A. BRESSAN and JULIO A. LUNA

INTEC[1]
C.C. 91
3000-Sante Fe, Argentina

PAUL A. CARROAD and ALFRED W. WILSON

Department of Food Science and Technology
University of California
Davis, California

Received for Publication July 1, 1981
Accepted for Publication March 21, 1983

ABSTRACT

A calculation method for batch washing of cottage cheese curd which yields combinations of washing time and ratio of water volume to curd volume is presented. The method is based on a theoretical model of the washing process which showed mass transfer of whey solids, rather than heat transfer, to be the rate limiting step. Input values include initial and final values of total solids concentration in the whey entrapped in the curd, and curd and water temperatures. Selection of optimum time and water volume depends on subsequent economic analysis.

INTRODUCTION

The washing of cottage cheese curd achieves the cooling of curd from cooking temperature to a lower temperature at which keeping quality is enhanced and the leaching of undesirable whey components from the curd particles (Emmons and Tuckey 1967). Washing may be accomplished as a series of batch operations with progressively colder water

[1]Institute of Technological Development for the Chemical Industry—Universidad Nacional del Litoral (UNL) and CONICET.

Journal of Food Process Engineering 7 (1983) 63-76.

(Emmons and Tuckey 1967) or as a semi-continuous operation (Hinds 1971). In either case, there is a trade-off between time of washing and the amount of water used. One may operate with much water and a short contact time between water and curd, or with less water over an extended washing cycle. This paper presents a method for determining such combinations of washing time and amount of water, the optimum combination depending upon an economic analysis.

The method specifically concerns batchwise washing of curd, in which curd and water are contacted in stages until the process is complete. The theoretical background which treats the washing process as a simultaneous heat and mass transfer phenomenon is detailed elsewhere (Bressan *et al.* 1981 and 1982; and Bressan and Carroad 1982). It was shown that the rate limiting process in washing is the diffusion of whey components from curd, since the heat transfer process is much more rapid (Bressan and Carroad 1982). A mass transfer model was developed for isothermal diffusion of whey solids from curd particles in a well-stirred system without chemical reaction. Spherical geometry of curd particles proved superior to cubical or cylindrical geometry (Bressan *et al.* 1982). The isothermal model was extended to washing at various temperatures in the range 25°C to 58°C, and an empirical correlation for effective diffusion coefficient of total solids from curd was determined (Bressan *et al.* 1981). The correlation is $D_{TS} = (0.0658T + 1.72) \times 10^{-6}$, where D_{TS} is in cm^2/s and T is in degrees C. The complete model, including considerations of diffusivity as a function of temperature, forms the basis of this work.

THEORY AND MODEL DEVELOPMENT

The model assumes a well stirred isothermal batch washing system containing a known amount of curd and water. The general equation of continuity for diffusion of component "i" is (Bressan *et al.* 1982):

$$\frac{\partial [C_i]^\gamma}{\partial t} = D^i_{eff} \cdot (\nabla^2 [C_i]^\gamma) \tag{1}$$

Assuming spherical geometry for curd particles, Eq. 1 becomes:

$$\frac{\partial [C_i]^\gamma}{\partial t} = D^i_{eff} \cdot \left(\frac{\partial^2 [C_i]^\gamma}{\partial r^2} + \frac{2}{r} \cdot \frac{\partial [C_i]^\gamma}{\partial r} \right) \tag{2}$$

where γ represents the phase of whey trapped within the curd. The initial and boundary conditions are:

$$\text{at } t = 0, \text{ at any } r, \quad [C_i]^{\gamma} = [C^{\circ}{}_i]^{\gamma} \tag{3}$$

$$\text{at } r = 0, \text{ at any time}, \quad \frac{\partial [C_i]^{\gamma}}{\partial r} = 0 \tag{4}$$

$$\text{at } r = a, \text{ at any time}, \quad V_{\mu} \cdot \frac{\partial [C_i]^{\mu}}{\partial t} = -\beta\gamma . 4\pi n a^2 D^{i}{}_{eff} \cdot \frac{\partial [C_i]^{\gamma}}{\partial r} \tag{5}$$

Whey solids are comprised of numerous components from low molecular weight salts to whey proteins. For simplicity, a lumped parameter analysis (Bailey 1975) can be used in which all solids are represented by the single pseudocomponent "total solids" (TS) and the diffusivity of this single pseudocomponent is defined as:

$$D_{TS} = \frac{\int_{\circ}^{\infty} [C^{\infty}{}_i]^{\gamma} (D^{i}{}_{eff}) \cdot D^{i}{}_{eff} \cdot dD^{i}{}_{eff}}{\int_{\circ}^{\infty} [C^{\infty}{}_i]^{\gamma} (D^{i}{}_{eff}) \cdot dD^{i}{}_{eff}} \tag{6}$$

The solution of Eq. (2) through (6) is given by Crank (1975) as:

$$[C_{TS}(t,r)]^{\gamma} = -\frac{[C^{\circ}{}_{TS}]^{\gamma}}{1+\alpha}\left[1 - \alpha \sum_{n=1}^{\infty} \frac{6(1+\alpha)}{9 + 9\alpha + \alpha^2 q_n^2} \cdot \frac{a}{r} \cdot \frac{\sin (q_n \cdot r/a)}{\sin q_n} \cdot e^{-D_{TS} \cdot q^2{}_n \cdot t/a^2}\right] \tag{7}$$

where the q_n's are the nonzero roots of:

$$\tan q_n = \frac{3q_n}{3 + \alpha \cdot q_n^2} \tag{8}$$

and α is defined as:

$$\alpha = \frac{V_{\mu}}{V_{\gamma}} \tag{9}$$

and $V_{\gamma} = \beta \cdot V_{\text{curd}}$.

The parameter β is the fraction of curd volume occupied by whey and is defined as:

$$\beta = \frac{[C^{\infty}{}_{TS}]^{\mu}(V_{\mu}/V_{\text{curd}})}{[C^{\circ}{}_{TS}]^{\gamma} - [C^{\infty}{}_{TS}]^{\mu}} \tag{10}$$

In calculating β it is assumed that the volume of liquid within the curd particle is constant and independent of temperature over the range of

washing temperatures. For the data previously presented (Bressan *et al.* 1982), $\alpha = 9.65$, $[C^{\infty}{}_{TS}]^{\mu} = 0.62\%$, $[C^{\circ}{}_{TS}]^{\gamma} = 6.6\%$, and so $\beta = 0.825$.

The theoretical concentration profiles given by Eq. (7) and taking $\alpha = 9.65$ are shown in Fig. 1.

The integrated form of Eq. (7) gives the mass relationship of total solids in the liquid phase surrounding the curd particles (denoted μ-phase) as (Crank 1975):

$$\left(\frac{M_{TS}(t)}{M^{\infty}{}_{TS}} \right)^{\mu} = 1 - \sum_{n=1}^{\infty} \frac{6\alpha(1+\alpha)}{9 + 9\alpha + \alpha^2 q_n^2} \cdot e^{-(D_{TS} \cdot q^2{}_n \cdot t/a^2)} \tag{11}$$

A series of mass balances performed over the system at different times, gives the following expressions:

$$(M^{\infty}{}_{TS})^{\mu} = [C^{\circ}{}_{TS}]^{\gamma} \cdot V_{\gamma} \cdot \left(\frac{\alpha}{1+\alpha} \right) \tag{12}$$

$$[M_{TS}(t)]^{\mu} = V_{\gamma}\{[C^{\circ}{}_{TS}]^{\gamma} - [C_{TS}(t)]^{\gamma}\} \tag{13}$$

Combining the results of Eq. (12) and (13) a simple relationship between dimensionless mass and concentration ratios can be obtained:

$$\left(\frac{M_{TS}(t)}{M^{\infty}{}_{TS}} \right)^{\mu} = \left[1 - \frac{[C_{TS}(t)]^{\gamma}}{[C^{\circ}{}_{TS}]^{\gamma}} \right] \left(\frac{1+\alpha}{\alpha} \right) \tag{14}$$

From Eq. (11) and (14) one obtains:

$$\frac{[C_{TS}(t)]^{\gamma}}{[C^{\circ}{}_{TS}]^{\gamma}} = \frac{1}{1+\alpha} + \sum_{n=1}^{\infty} \frac{6\alpha^2}{9 + 9\alpha + \alpha^2 q_n^2} \exp(-D_{TS} q_n^2 t/a^2) \tag{15}$$

Figure 2 illustrates the relationship between the dimensionless concentration ratio as a function of $D_{TS} \cdot t/a^2$ for values of α between 0.2 and 10.0.

The proposed model assumes diffusion in the solid as the controlling factor of the leaching process, neglecting any external resistance.

The extent of that control can be evaluated by means of the Biot number defined as (Schwartzberg and Chao 1982):

$$Bi = \frac{k_e \cdot a}{\beta \cdot D_{TS}} \tag{16}$$

The external mass transfer coefficient k_e has been evaluated by using the following expression (Brian and Hales 1969):

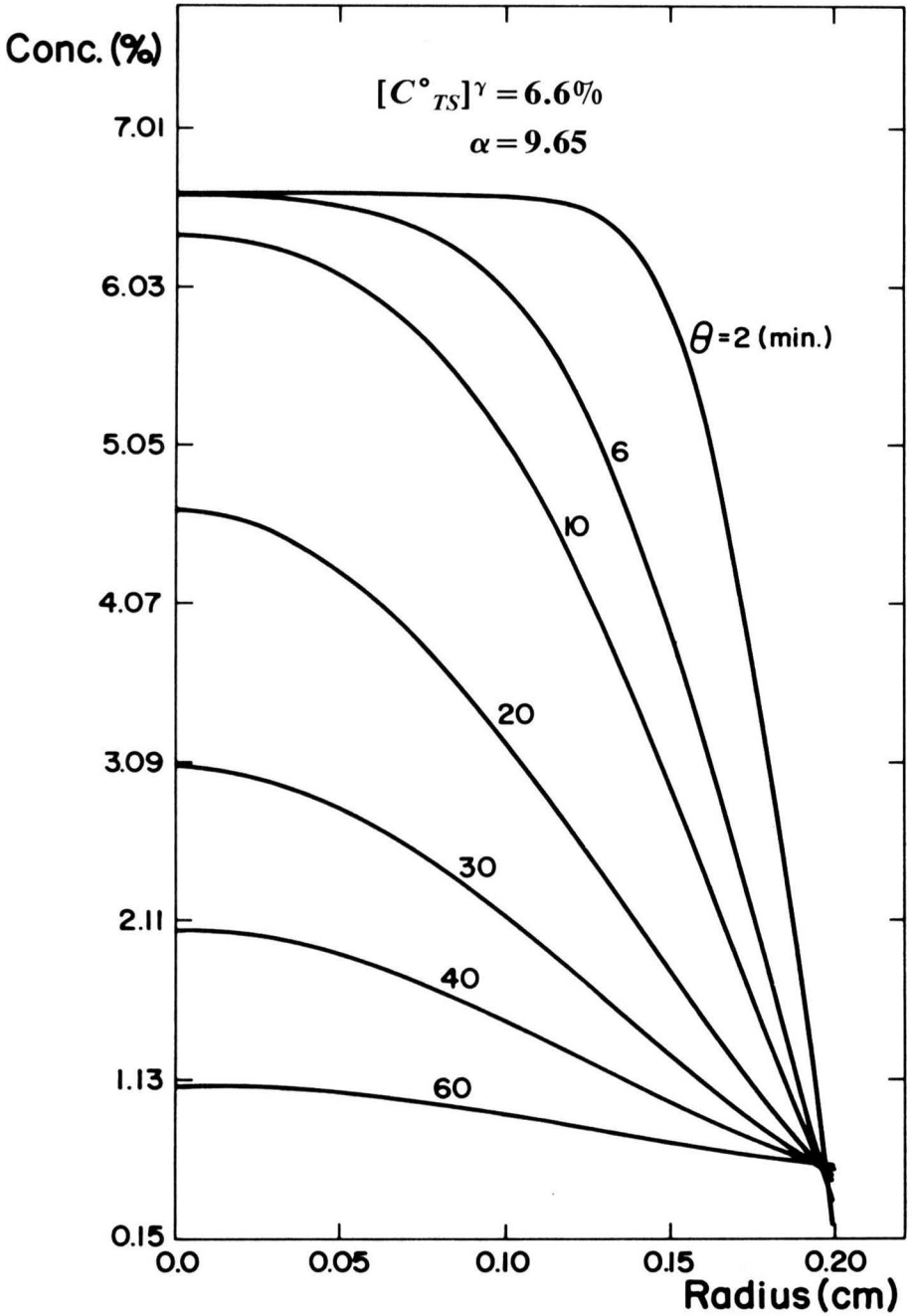

FIG. 1. RADIAL CONCENTRATION PROFILES FOR A SPHERICAL CURD PARTICLE

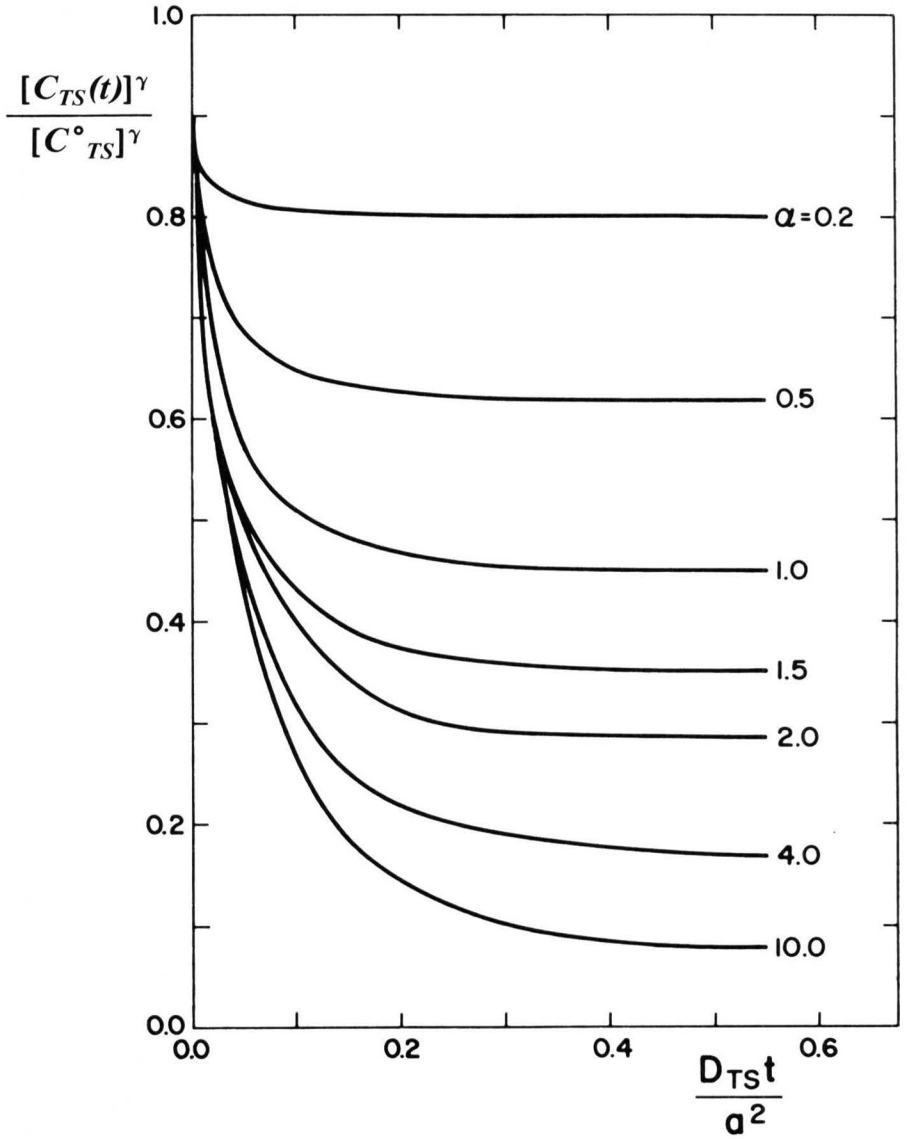

FIG. 2. DIMENSIONLESS CONCENTRATION RATIO AS A FUNCTION OF $D_{TS}\ t/a^2$ FOR SEVERAL VALUES OF α, CALCULATED FROM EQ. (15)

$$\frac{S_h}{S_c^{1/3}} = \left(\frac{d^4_p \cdot P/m}{\nu^3} \right)^{1/3} \tag{17}$$

Then:

$$k_e = \left(\frac{dp \cdot P/m \cdot D^2}{\nu^2} \right)^{1/3} \tag{18}$$

By calculating P/m from a power number correlation (Foust *et al.* 1960) and using the value of D_L for lactose, the main diffusing component at 25°C (Schwartzberg and Chao 1982) the resulting k_e value is 3.03×10^{-4} m/s. For $\beta = 0.825$, $a = 1.89 \times 10^{-3}$ m and $D_{TS} = 0.34 \times 10^{-9}$ m^2/s. (Bressan *et al.* 1982), the Biot number is approximately 2×10^3. This value of the Biot number indicates the validity of assuming negligible external resistance.

The degree of agitation under which the parameters β, a, and D_{TS} were evaluated was such as to maintain all the particles suspended in the liquid. This experimental criterion should be satisfied in any other system to which the model is applied for the assumption of negligible external resistance to be valid.

Performing a simple mass balance over the system, and using Eq. 15, the theoretical concentration of total solids at time "t" in the μ-phase can be expressed as:

$$[C_{TS}(t)]^{\mu} = [C^{\circ}{}_{TS}]^{\gamma} \left(\frac{1}{1+\alpha} - \sum_{n=1}^{\infty} \frac{6\alpha}{9 + 9\alpha + \alpha^2 q_n^2} \exp[-D_{TS} q_n^2 t/a^2] \right) \tag{19}$$

Figure 3 shows $[C_{TS}(t)]^{\mu}$ calculated by Eq. (19) and the corresponding $[C_{TS}(t)]^{\mu}{}_{\text{exp}}$ experimental values which were presented previously (Bressan *et al.* 1982).

The initial condition Eq. (3) needed for solution of Eq. (2) requires specification of an initial concentration profile of total solids within the curd particle. Before the first washing, the initial concentration profile is uniform or homogeneous across the particle. For subsequent washings, the initial concentration profile is homogeneous only if sufficient time has elapsed for mass transfer equilibrium to be achieved. Otherwise, the concentration profile $[C_{TS}(r,\theta)]^{\gamma}$ resulting from one washing should be used as the initial condition in Eq. (3) for the next washing. For example, Fig. 1 shows the concentration profile at any time as predicted by Eq. (7) for the first washing which can be applied as an initial condition to the second washing.

The time needed for the concentration profile within a curd particle to become radially homogeneous (i.e., flat) can be calculated rigorously by solving Eq. (2) with the following initial and boundary conditions:

I.C.:
at $t = 0$

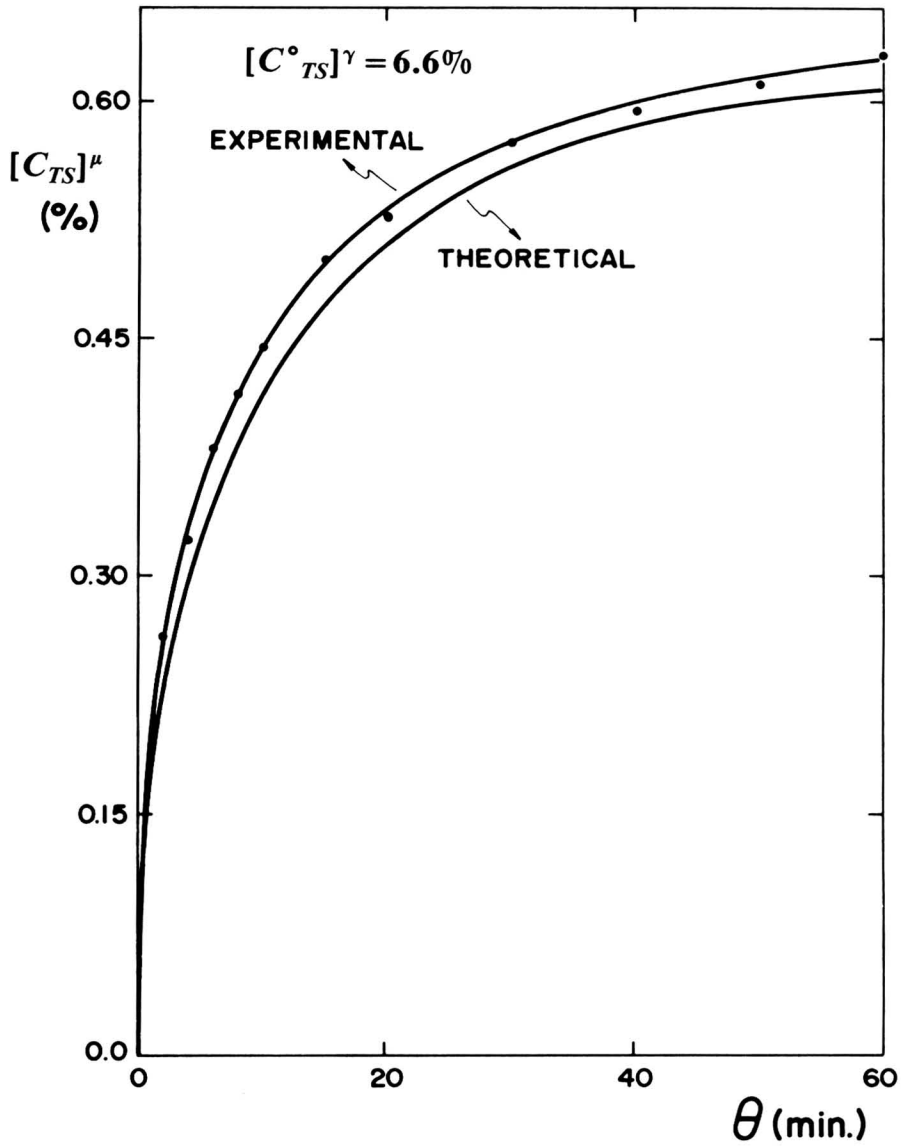

FIG. 3. THEORETICAL (Eq. (19)) AND EXPERIMENTAL TS CONCENTRATIONS IN THE μ-PHASE AS A FUNCTION OF WASHING TIME

$[C_{TS}(r,\theta)]^{\gamma}$ as given by Eq. (7)

B.C.:

1) At $r=0$, for any time

$$\left.\frac{\partial[C_{TS}]^{\gamma}}{\partial r}\right|_{r=0} = 0 \tag{20}$$

2) At $r=a$, for any time

$$\left.\frac{\partial[C_{TS}]^{\gamma}}{\partial r}\right|_{r=0} = 0 \tag{21}$$

The solution is:

$$[C_{TS}(r,t)]^{\gamma} = \frac{A_o}{2} + \sum_{m=1}^{\infty} A_m \sin(\lambda_m r/a) \cdot \frac{a}{r} \exp(-\lambda_m^2 D_{TS} t/a^2) \tag{22}$$

where the λ_m's are the nonzero roots of

$$\tan \lambda_m = \lambda_m \ . \tag{23}$$

The $A_o/2$ term is:

$$\frac{A_o}{2} = \frac{[C^{\circ}{}_{TS}]^{\gamma}}{1+\alpha}\left[1 - 18\alpha(1+\alpha)\sum_{n=1}^{\infty}\frac{1}{9+9\alpha+\alpha^2 q_n^2}\frac{1}{\sin q_n}\left(\frac{\sin q_n}{q_n^2} - \cos\frac{\cos q_n}{q_n}\right)\cdot\exp(-D_{TS}q_n^2\theta/a^2)\right] \tag{24}$$

and the A_m's are:

$$A_m = -\left(\sum_{n=1}^{\infty}\frac{6\alpha[C_o]^{\gamma}}{9+9\alpha+\alpha^2 q_n^2}\cdot\frac{\sin\lambda_m}{\sin q_n}\cdot\frac{(\sin q_n - q_n\cos q_n)}{(q_n^2-\lambda_m^2)}\cdot\exp(-D_{TS}q_n^2\theta/a^2)\right) \div \left(\frac{1}{2} - \frac{\sin 2\lambda_m}{4\lambda_m}\right) \tag{25}$$

Figure 4 shows the concentration profiles of Eq. (22) tending toward equilibrium for the experimental conditions used in these studies (Bressan *et al.* 1981 and 1982; Bressan and Carroad 1982): $\alpha=9.65$, $\theta=20$ min, $a=1.89\times10^{-3}$ m, $[C_{TS}{}^{\circ}]=6.6\%$. The flat profile corresponds to a uniform liquid-phase concentration of total solids inside the particle that is equal to $A_o/2$. From the data given and using Eq. (24), the value of $A_o/2$ which is obtained is 1.81%. This value was confirmed experimentally by extracting whey by centrifugation (20,000 g for 10 min) from curd that had been washed for 20 min. The mean of four mea-

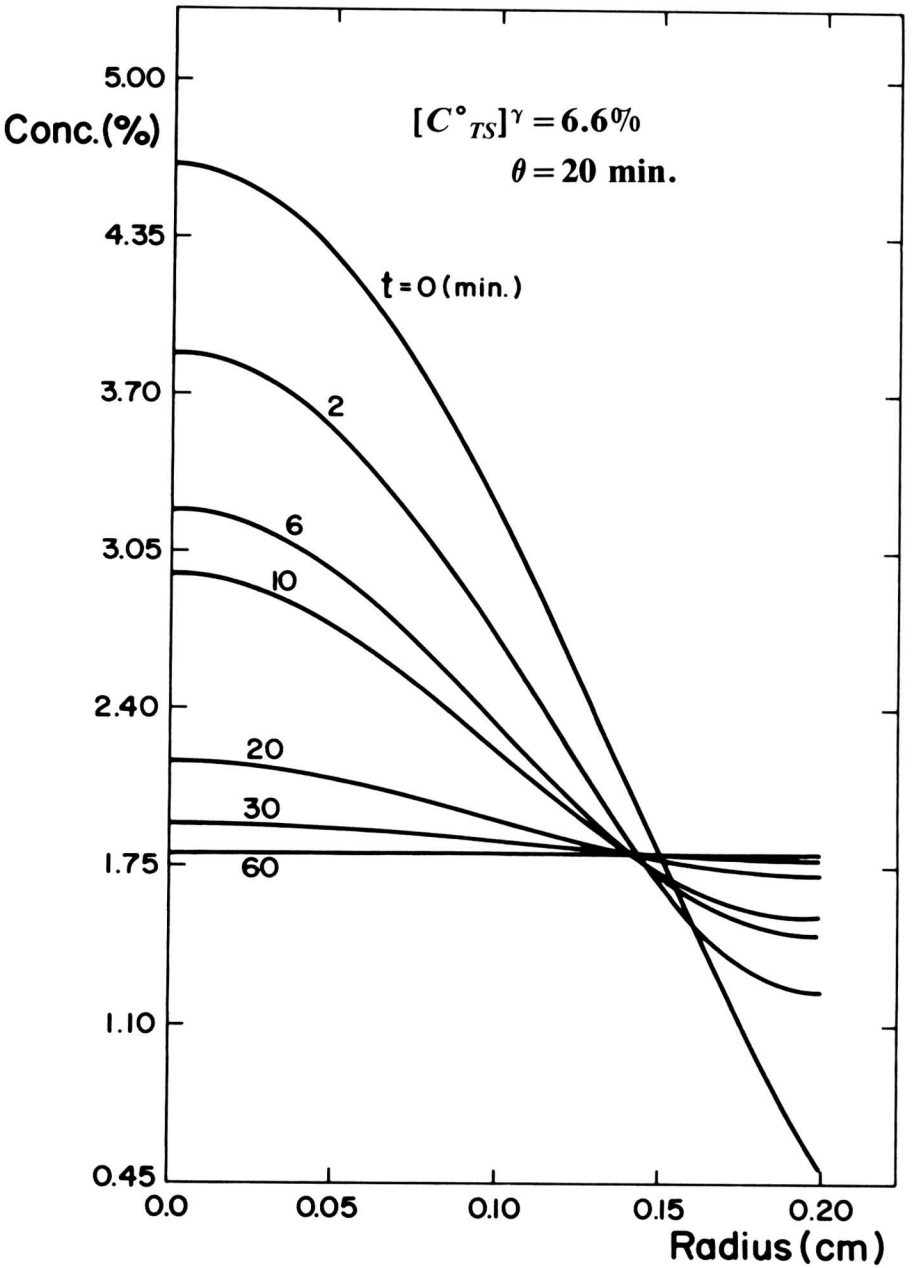

FIG. 4. EVOLUTION OF THE CONCENTRATION PROFILES (Eq. (22)) FOR THE EXPERIMENTAL CONDITIONS $\mu = 9.65$, $\theta = 20$ MIN, $a = 1.89 \times 10^{-3}$ M, AND [C°TS] = 6.6%

surements of total solids concentration was 2.14%, which shows acceptable agreement.

Although in theory the time required for Eq. (22) to achieve a flat profile (i.e., equilibrium) is infinite, a more practical approach is to consider washing complete when the liquid phase total solids concentration at the center of the particle is within 10% of the $A_o/2$ value. For the experimental case described, this condition is achieved at 27 min. Such a duration is of the order of magnitude of that typically required for one complete batch washing cycle (Dunkley and Patterson 1977; Emmons and Tuckey 1967) which suggests the applicability of the method to industrial practice.

Previous work (Bressan and Carroad 1982) established that heat transfer can be neglected in washing with respect to mass transfer and that the mass transfer aspect of the washing process can be treated isothermally. The temperature at which washing occurs is defined as:

$$T_f = \frac{T^\circ_c - T^\circ_w \cdot K}{K + 1} \tag{26}$$

where

$$K = \frac{M_{\text{water}} \cdot C^w}{M_{\text{curd}} \cdot C^c}$$

is the ratio of the heat capacity of the liquid used for washing to that of the curd.

Equation (15) is the principal equation to be used for calculational purposes and is expressed graphically in Fig. 2 to facilitate its use. The empirical correlation for diffusivity as a function of temperature and Eq. (26) are auxiliary equations to be used to determine the washing temperature and the effective diffusivity at that temperature.

Method of Calculation

The methodology presented here yields a time of batch washing, t, and an associated volume ratio of water to whey trapped inside the curd particle, α, necessary to reduce the concentration of whey solids in curd from an initial value $[C^\circ_{TS}]^\gamma$ to some final value $[C_{TS}(t)]^\gamma$. The magnitude of this final value must be determined by the processor as a trade-off between consumer acceptance which presumably favors a low concentration of total solids and waste treatment cost which favors a

high concentration of solids in the curd and decreased effluent concentration.

The resultant time and water volume allows cost estimation based on equipment sizing, labor, water supply and treatment, refrigeration load, etc. An iterative procedure of assigning costs to each t and α combination followed by economic analysis will indicate the most economical design combination for any system.

Parameters which serve as inputs are β, C^c, a, $[C^\circ_{TS}]^\gamma$, $[C_{TS}(t)]^\gamma$, and T°_c. There is some freedom of choice with respect to T°_w and M_{curd}. The calculation methodology is as follows depending upon whether one first assumes the value for t or α.

Case I. Fix α and calculate t.

Step 1: Calculate $[C_{TS}(t)]^\gamma/[C^\circ_{TS}]^\gamma$.
Step 2: With above ratio and α, determine $D_{TS}\cdot t/a^2$ from Fig. 2.
Step 3: Calculate T_f from Eq. (26).
Step 4: Calculate D_{TS} from empirical correlation:
$D_{TS}=(0.0658T+1.72)\times 10^{-6}$.
Step 5: Calculate t from $D_{TS}\cdot t/a^2$.

Case II. Fix t and calculate α.

Step 1: Calculate T_f from Eq. (26).
Step 2: Calculate D_{TS} from empirical correlation:
$D_{TS}=(0.0658T+1.72)\times 10^{-6}$.
Step 3: Calculate $D_{TS}\cdot t/a^2$.
Step 4: Calculate $[C_{TS}(t)]^\gamma/[C^\circ_{TS}]^\gamma$.
Step 5: With above ratio and $D_{TS}\cdot t/a^2$, determine α from Fig. 2.

This method permits one to select either a nonequilibrium or an equilibrium concentration of whey solids during batch washing and permits the calculation of values of other relevant parameters such as M°_{TS}, M^∞_{TS}, $[C^\infty_{TS}]^\gamma$, $[C^\infty_{TS}]^\mu$, etc.

NOMENCLATURE

a = radius of the curd particle, cm
Bi = Biot number
C^c = specific heat of curd
C^w = specific heat of water
$[C_i]^\gamma$ = concentration of component "i"

$[C^{\infty}_{i}]^{\mu} = [C^{\infty}_{i}]^{\gamma}$ = concentration of component "i" at infinite time
$[C^{\circ}_{TS}]^{\gamma}$ = initial concentration of total solids
$[C^{\infty}_{TS}]^{\mu} = [C^{\infty}_{TS}]^{\gamma}$ = concentration of total solids at infinite time
$[C_{TS}(t)]^{\gamma}$ = concentration of total solids at time "t"
d_p = particle diameter, cm
D^{i}_{eff} = diffusion coefficient of component "i", cm^2/s
D_{TS} = effective diffusion coefficient of total solids, cm^2/s
k_e = external mass transfer coefficient, cm/s
K = ratio of the heat capacity of the fluid to that of the curd
$M_{curd} = M_c$ = curd mass, g
M_w = water mass, g
M°_{TS} = initial mass of total solids, g
$M_{TS}(t)$ = mass of total solids at time "t", g
M^{∞}_{TS} = mass of total solids at infinite time, g
n = number of curd particles
q_n = nonzero root of the transcendental Eq. (8)
r = radius of the particles, cm
Sh = Sherwood number
Sc = Schmidt number
t = time, s
T = temperature, °C
T_f = final system temperature, °C
T°_{c} = initial curd temperature, °C
T°_{w} = initial water temperature, °C
V_{γ} = volume of the γ-phase, cm^3
V_{μ} = volume of the μ-phase, cm^3
α = volume of wash water/volume of liquid trapped inside the particles
β = porosity
ν = kinematic viscosity, m^2/s
λ_m = nonzero roots of the transcendental Eq. (23)
$\rho_{curd} = \rho_c$ = density of the curd, g/cm^3
γ = whey trapped phase
μ = wash water phase
θ = washing time (min)

ACKNOWLEDGMENTS

The authors acknowledge useful discussions with Professors R. L. Merson and W. L. Dunkley of the Department of Food Science and

Technology, University of California at Davis. This project was supported by the University of California Agricultural Experiment Station (Project 3610-H).

REFERENCES

BAILEY, J. E. 1975. Diffusion of grouped multicomponent mixtures in uniform and nonuniform media AIChE J. *21*(1), 192.

BRESSAN, J. A., CARROAD, P. A., MERSON, R. L., and DUNKLEY, W. L. 1981. Temperature dependence of effective diffusion coefficient for total solids during washing of cheese curd. J. Food Sci. *46*(6), 1958.

BRESSAN, J. A., CARROAD, P. A., MERSON, R. L., and DUNKLEY, W. L. 1982. Modelling of isothermal diffusion of whey components from small curd cottage cheese during washing. J. Food Sci. *47*(1), 84.

BRESSAN, J. A. and CARROAD, P. A. 1982. Heat transfer modelling of the washing of small curd cottage cheese. J. Food Sci. *47*(1), 89.

BRIAN, P. L. T. and HALES, H. B. 1969. Effects of transpiration and changing diameter on heat and mass transfer to spheres. AIChE J. *15*, 419.

CRANK, J. 1975. *The Mathematics of Diffusion.* Oxford University Press, London.

DUNKLEY, W. L. and PATTERSON, D. R. 1977. Relations among manufacturing procedures and properties of cottage cheese. J. Dairy Science *60*(11), 1824.

EMMONS, D. B. and TUCKEY, S. L. 1967. Cottage cheese and other cultured milk products. Pfizer, New York.

FOUST, A. S. 1960. *Principles of Unit Operations.* John Wiley & Sons, Inc., New York.

HINDS, H. Jr. 1971. Cottage cheese curd washing and handling. Cultured Dairy Products J. *6*(2), 21.

SCHWARTZBERG, H. G. and CHAO, R. G. 1982. Solute diffusivities in leaching processes. J. Food Tech. *36*(2), 73.

F N P

JOURNALS AND BOOKS IN FOOD SCIENCE AND NUTRITION

Journals

JOURNAL OF NUTRITION, GROWTH AND CANCER, G. P. Tryfiates

JOURNAL OF FOOD SERVICE SYSTEMS, O. P. Snyder, Jr.

JOURNAL OF FOOD BIOCHEMISTRY, H. O. Hultin, N. F. Haard and J. R. Whitaker

JOURNAL OF FOOD PROCESS ENGINEERING, D. R. Heldman

JOURNAL OF FOOD PROCESSING AND PRESERVATION, T. P. Labuza

JOURNAL OF FOOD QUALITY, M. P. De Figueiredo

JOURNAL OF FOOD SAFETY, M. Solberg and J. D. Rosen

JOURNAL OF TEXTURE STUDIES, P. Sherman and M. C. Bourne

Books

PRODUCT TESTING AND SENSORY EVALUATION OF FOODS
H. R. Moskowitz

SHELF-LIFE DATING OF FOODS
T. P. Labuza

ANTINUTRIENTS AND NATURAL TOXICANTS IN FOOD
R. L. Ory

UTILIZATION OF PROTEIN RESOURCES
D. W. Stanley, E. D. Murray and D. H. Lees

FOOD INDUSTRY ENERGY ALTERNATIVES
R. P. Ouellette, N. W. Lord and P. E. Cheremisinoff

VITAMIN B_6: METABOLISM AND ROLE IN GROWTH
G. P. Tryfiates

HUMAN NUTRITION, 3RD ED.
R. F. Mottram

DIETARY FIBER: CURRENT DEVELOPMENTS OF IMPORTANCE TO HEALTH
K. W. Heaton

RECENT ADVANCES IN OBESITY RESEARCH II
G. A. Bray

FOOD POISONING AND FOOD HYGIENE, 4TH ED.
B. C. Hobbs and R. J. Gilbert

POSTHARVEST BIOLOGY AND BIOTECHNOLOGY
H. O. Hultin and M. Milner

THE SCIENCE OF MEAT AND MEAT PRODUCTS, 2ND ED.
J. F. Price and B. S. Schweigert

U.S. POSTAL SERVICE

STATEMENT OF OWNERSHIP, MANAGEMENT AND CIRCULATION

(Required by 39 U.S.C. 3685)

1. TITLE OF PUBLICATION	A. PUBLICATION NO.	2. DATE OF FILING
Journal of Food Process Engineering	0 1 4 5 8 8 7 6	Oct. 1, 1983
3. FREQUENCY OF ISSUE	**A. NO. OF ISSUES PUBLISHED ANNUALLY**	**B. ANNUAL SUBSCRIPTION PRICE**
Quarterly	4	$60.00

4. LOCATION OF KNOWN OFFICE OF PUBLICATION *(Street, City, County, State and ZIP Code) (Not printers)*
155 Post Road East, Suite 6, POB 71, Westport, Fairfield, CT 06881

5. LOCATION OF THE HEADQUARTERS OR GENERAL BUSINESS OFFICES OF THE PUBLISHERS *(Not printers)*
155 Post Road East, Suite 6 POB 71, Westport, Fairfield, CT 06881

6. NAMES AND COMPLETE ADDRESSES OF PUBLISHER, EDITOR, AND MANAGING EDITOR

PUBLISHER *(Name and Address)*
John J. O'Neil, 155 Post Road East, Suite 6, POB 71, Westport, CT 06881

EDITOR *(Name and Address)*
Dr. Dennis R. Heldman, Michigan State University, Dept. of Food Science & Human

MANAGING EDITOR *(Name and Address)* Nutrition, E. Lansing, MI 48823

7. OWNER *(If owned by a corporation, its name and address must be stated and also immediately thereunder the names and addresses of stockholders owning or holding 1 percent or more of total amount of stock. If not owned by a corporation, the names and addresses of the individual owners must be given. If owned by a partnership or other unincorporated firm, its name and address, as well as that of each individual must be giving. If the publication is published by a nonprofit organization, its name and address must be stated.)*

NAME	ADDRESS
Food & Nutrition Press, Inc.	155 Post Road East, POB 71, Westport, CT 06881
Technomic Publishing Co	851 New Holland Avenue, Box 3535, Lancaster, PA
(Melvyn A. Kohudic)	851 New Holland Ave.,Box 3535,Lancaster, PA 17604
John J.O'Neil	155 Post Road East,POB 71, Westport,CT 06881

8. KNOWN BONDHOLDERS, MORTGAGEES, AND OTHER SECURITY HOLDERS OWNING OR HOLDING 1 PERCENT OR MORE OF TOTAL AMOUNT OF BONDS, MORTGAGES OR OTHER SECURITIES *(If there are none, so state)*

NAME	ADDRESS
None	

9. FOR COMPLETION BY NONPROFIT ORGANIZATIONS AUTHORIZED TO MAIL AT SPECIAL RATES *(Section 132.122, PSM)*
The purpose, function, and nonprofit status of this organization and the exempt status for Federal income tax purposes *(Check one)*

☐ HAVE NOT CHANGED DURING PRECEDING 12 MONTHS ☐ HAVE CHANGED DURING PRECEDING 12 MONTHS *(If changed, publisher must submit explanation of change with this statement.)*

10. EXTENT AND NATURE OF CIRCULATION	AVERAGE NO. COPIES EACH ISSUE DURING PRECEDING 12 MONTHS	ACTUAL NO. COPIES OF SINGLE ISSUE PUBLISHED NEAREST TO FILING DATE
A. TOTAL NO. COPIES PRINTED *(Net Press Run)*	475	450
B. PAID CIRCULATION 1. SALES THROUGH DEALERS AND CARRIERS, STREET VENDORS AND COUNTER SALES	0	0
2. MAIL SUBSCRIPTIONS	310	305
C. TOTAL PAID CIRCULATION *(Sum of 10B1 and 10B2)*	310	305
D. FREE DISTRIBUTION BY MAIL, CARRIER OR OTHER MEANS SAMPLES, COMPLIMENTARY, AND OTHER FREE COPIES	25	26
E. TOTAL DISTRIBUTION *(Sum of C and D)*	335	331
F. COPIES NOT DISTRIBUTED 1. OFFICE USE, LEFT OVER, UNACCOUNTED, SPOILED AFTER PRINTING	140	119
2. RETURNS FROM NEWS AGENTS	0	0
G. TOTAL *(Sum of E, F1 and 2—should equal net press run shown in A)*	475	450

11. I certify that the statements made by me above are correct and complete.

SIGNATURE AND TITLE OF EDITOR, PUBLISHER, BUSINESS MANAGER, OR OWNER
John J. O'Neil, Publisher

12. FOR COMPLETION BY PUBLISHERS MAILING AT THE REGULAR RATES *(Section 132.121, Postal Service Manual)*

39 U. S. C. 3626 provides in pertinent part: "No person who would have been entitled to mail matter under former section 4359 of this title shall mail such matter at the rates provided under this subsection unless he files annually with the Postal Service a written request for permission to mail matter at such rates."

In accordance with the provisions of this statute, I hereby request permission to mail the publication named in Item 1 at the phased postage rates presently authorized by 39 U. S. C. 3626.

SIGNATURE AND TITLE OF EDITOR, PUBLISHER, BUSINESS MANAGER, OR OWNER
John J. O'Neil, Publisher

(See instructions on reverse)

GUIDE FOR AUTHORS

Typewritten manuscripts in triplicate should be submitted to the editorial office. The typing should be double-spaced throughout with one-inch margins on all sides.

Page one should contain: the title, which should be concise and informative; the complete name(s) of the author(s); affiliation of the author(s); a running title of 40 characters or less; and the name and mail address to whom correspondence should be sent.

Page two should contain an abstract of not more than 150 words. This abstract should be intelligible by itself.

The main text should begin on page three and will ordinarily have the following arrangement:

Introduction: This should be brief and state the reason for the work in relation to the field. It should indicate what new contribution is made by the work described.

Materials and Methods: Enough information should be provided to allow other investigators to repeat the work. Avoid repeating the details of procedures which have already been published elsewhere.

Results: The results should be presented as concisely as possible. Do not use tables *and* figures for presentation of the same data.

Discussion: The discussion section should be used for the interpretation of results. The results should not be repeated.

In some cases it might be desirable to combine results and discussion sections.

References: References should be given in the text by the surname of the authors and the year. *Et al.* should be used in the text when there are more than two authors. All authors should be given in the Reference section. In the Reference section the references should be listed alphabetically. See below for style to be used.

DEWALD, B., DULANEY, J. T. and TOUSTER, O. 1974. Solubilization and polyacrylamide gel electrophoresis of membrane enzymes with detergents. In *Methods in Enzymology,* Vol. xxxii, (S. Fleischer and L. Packer, eds.) pp. 82–91, Academic Press, New York.

HASSON, E. P. and LATIES, G. G. 1976. Separation and characterization of potato lipid acylhydrolases. Plant Physiol. *57,* 142–147.

ZABORSKY, O. 1973. *Immobilized Enzymes,* pp. 28–46, CRC Press, Cleveland, Ohio.

Journal abbreviations should follow those used in *Chemical Abstracts.* Responsibility for the accuracy of citations rests entirely with the author(s). References to papers in press should indicate the name of the journal and should only be used for papers that have been accepted for publication. Submitted papers should be referred to by such terms as "unpublished observations" or "private communication." However, these last should be used only when absolutely necessary.

Tables should be numbered consecutively with Arabic numerals. The title of the table should appear as below:

Table 1. Activity of potato acyl-hydrolases on neutral lipids, galactolipids, and phospholipids

Description of experimental work or explanation of symbols should go below the table proper.

Figures should be listed in order in the text using Arabic numbers. Figure legends should be typed on a separate page. Figures and tables should be intelligible without reference to the text. Authors should indicate where the tables and figures should be placed in the text. Photographs must be supplied as glossy black and white prints. Line diagrams should be drawn with black waterproof ink on white paper or board. The lettering should be of such a size that it is easily legible after reduction. Each diagram and photograph should be clearly labeled on the reverse side with the name(s) of author(s), and title of paper. When not obvious, each photograph and diagram should be labeled on the back to show the top of the photograph or diagram.

Acknowledgments: Acknowledgments should be listed on a separate page.

Short notes will be published where the information is deemed sufficiently important to warrant rapid publication. The format for short papers may be similar to that for regular papers but more concisely written. Short notes may be of a less general nature and written principally for specialists in the particular area with which the manuscript is dealing. Manuscripts which do not meet the requirement of importance and necessity for rapid publication will, after notification of the author(s), be treated as regular papers. Regular papers may be very short.

Standard nomenclature as used in the engineering literature should be followed. Avoid laboratory jargon. If abbreviations or trade names are used, define the material or compound the first time that it is mentioned.

EDITORIAL OFFICE: Prof. D. R. Heldman, Editor, Journal of Food Process Engineering, Michigan State University, Department of Food Science and Human Nutrition, East Lansing, Michigan 48824 USA.

JOURNAL OF FOOD PROCESS ENGINEERING VOL. 7 NO. 1

CONTENTS